

JOURNAL OF FLOW CHEMISTRY (ISSN: 2062-249X) (eISSN: 2063-0212) 4: (3) pp. 125-134. (2014)

DOI: 10.1556/JFC-D-14-00011

# Lipase-catalyzed kinetic resolution of 1-(2-hydroxycyclohexyl)indoles in batch and continuous-flow systems

Péter Falus<sup>1</sup>, Zoltán Boros<sup>1,2</sup>, Péter Kovács<sup>3</sup>, László Poppe<sup>1,2\*</sup>, József Nagy<sup>1,2\*</sup>

<sup>1</sup>*Department of Organic Chemistry and Technology, Budapest University of Technology and Economics, H-1111 Budapest, Műegyetem rkp. 3., Hungary*

<sup>2</sup>*SynBiocat Ltd., H-1173 Budapest, Lázár deák u. 4/1., Hungary*

<sup>3</sup>*Research Centre for Natural Sciences, Institute of Organic Chemistry, Hungarian Academy of Sciences, H-1117 Budapest, Magyar tudósok körútja 2., Hungary*

## ABSTRACT

The lipase catalysed kinetic resolution of three *trans*-1-(2-hydroxycyclohexyl)-indoles in both batch and continuous-flow systems is reported. Ring opening of cyclohexene oxide by the corresponding indole followed by enzymatic acylation with vinyl acetate resulted in novel, highly enantioenriched indole-substituted cyclohexanols and cyclohexyl acetates. The effect of the temperature on enantiomeric ratio (*E*) and productivity (specific reaction rate,  $r_{flow}$ ) in the continuous-flow mode acylation was studied at analytical scale in the 0–70°C range. Preparative scale kinetic resolution of the three indole derivatives was performed in mixed continuous- and recirculation-flow mode resulting in almost complete conversion and good to excellent enantiomeric purity of the products.

**Keywords:** Lipase, heterocyclic secondary alcohol, kinetic resolution, continuous-flow biotransformation, enantiomer selectivity, temperature effect

## 1. Introduction

Indole derivatives are important as natural compounds and utilized not only in the pharmaceutical industry but also used in agrochemicals (e.g. fungicides, herbicides), in dietary supplements and nutraceuticals, colorants industry or fragrance industry.<sup>1,2</sup> Substituted

---

\* Corresponding authors. Department of Organic Chemistry and Technology, Budapest University of Technology and Economics, H-1111 Budapest, Műegyetem rkp. 3., Hungary. Tel: +36 1 463 3299; fax: +36 1 463 3697

E-mail addresses: jnagy@mail.bme.hu (J. Nagy), poppe@mail.bme.hu (L. Poppe)

indole skeleton is a prevalent building block of numerous pharmaceutical agents. One of the reasons which make indole ring quite indispensable is the wide range of biological effects: e.g. the amino-acid tryptophan, the hormones serotonin<sup>3</sup> and melatonin<sup>4</sup>, the psychotropic drugs LSD,<sup>5</sup> bufotenine and psilocybin<sup>6</sup> and the antitumor agent vinblastine.<sup>7,8</sup>

Ring opening of epoxides with indole derivatives under neutral or basic conditions follows an S<sub>N</sub>2 mechanism and provide *trans*-1,2-disubstituted products.<sup>9</sup> These reactions usually require a strong base or acid,<sup>10</sup> high temperature<sup>11</sup> or high pressure.<sup>12</sup> Recently, epoxy ring opening under microwave condition<sup>13,14</sup> or in continuous-flow reactor<sup>15</sup> have been reported.

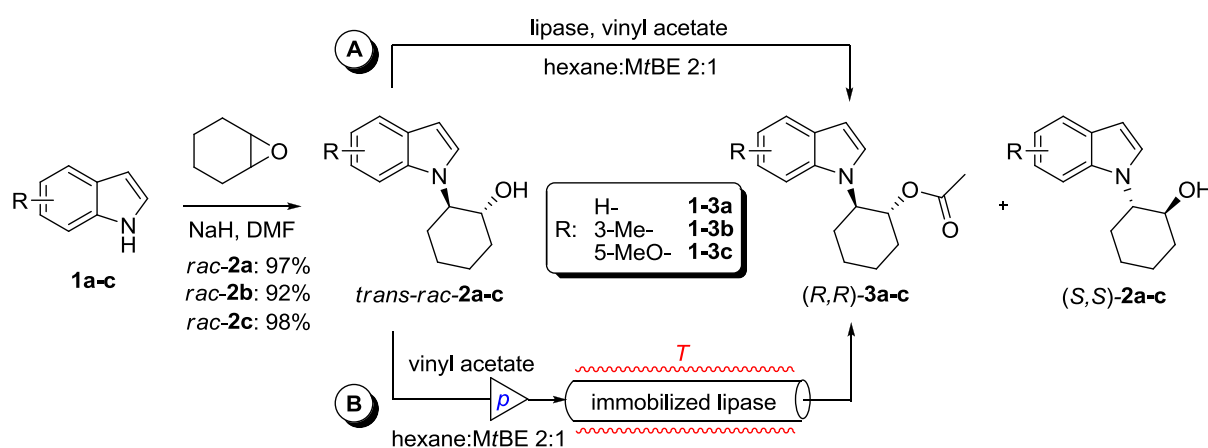
Due to the ever growing need of the pharmaceutical and fine chemicals industries for enantiomerically pure compounds, the armoury of novel stereoselective synthetic methods is continuously expanding. The use of biocatalysts for these purposes grows with this expansion<sup>16-19</sup> since biocatalysis often requires milder conditions in stereoselective reaction than chemocatalysis. Hydrolases, especially lipases are among the most often used enzymes for synthetic purposes.<sup>20</sup> Lipases have been used for numerous stereoselective biotransformations<sup>21-26</sup> such as kinetic resolution (KR)<sup>20,27</sup>, deracemisation and dynamic kinetic resolution (DKR)<sup>30</sup> due to their high regio-, chemo- and enantioselectivity, high stability, compatibility of organic solvents, wide substrate range, and because they do not need co-factors. Lipases – either in their native form or tailored by genetic engineering – are ideally suited for industrial applications,<sup>17,28</sup> preferably in their immobilised forms to enable recycling. Alcohols and amines are the most thoroughly investigated substrates in KR and DKR.<sup>29-38</sup> The production of chiral alcohols brought in 2002 more than 7 billion dollars in revenues worldwide and this was forecasted to be 14.9 billion dollars by the year 2009.<sup>39</sup>

Although a tremendous number of biocatalytic reactions have been studied,<sup>16-18,20-26</sup> the operational parameters reported for most of them seem to be rather suboptimal. Therefore, there is still much room for optimization promoting thereby faster transfer to an industrial scale. Even today, most of biosynthetic operations are performed as a fixed, batch based single step procedure. Although continuous processes offer several advantages – such as facile automation, reproducibility and safety – the benefits of the flow-through approach<sup>40-45</sup> have not been fully exploited so far.

Because immobilized biocatalysts are recyclable, storable and easy to handle, immobilization is an important trend in biotechnology.<sup>46-51</sup> Selectivity, specificity, catalytic activity and enzyme stability are key factors affecting the efficiency of biocatalysts.<sup>16-18,20-26</sup> Immobilization can often improve these key properties<sup>46-51</sup> and also enabling the use of biocatalysts under continuous-flow conditions.<sup>19</sup>

Among the factors influencing selectivity, catalytic activity and stability of the biocatalysts under continuous-flow conditions, temperature effects are the most important. In enzyme-catalysed reactions, increasing temperature generally decreases selectivity.<sup>52-62</sup> In a few studies, however, enhanced selectivity with increasing temperature,<sup>63,64</sup> or a maximum of enantioselectivity at a certain temperature,<sup>38,65</sup> or even indifference to temperature was found.<sup>66</sup> In most of the quoted examples, the enzyme-catalysed reactions were carried out in batch mode (in stirred or shaken flasks) and only a few studies on the temperature effects on lipase-catalysed KRs were performed in continuous-flow mode so far.<sup>19,38,65</sup>

Herein the synthesis and lipase-catalysed kinetic resolutions of racemic 1-(2-hydroxycyclohexyl)indoles (*rac-2a-c*) are reported in both batch and continuous-flow systems (Scheme 1). According to our best knowledge, these are the first KRs of the already known (*rac-2a*) and of the novel *trans*-1-(2-hydroxycyclohexyl)indoles (*rac-2b* and *rac-2c*). The effect of temperature on enantiomer selectivity was also investigated under continuous-flow conditions.



**Scheme 1.** Synthesis and kinetic resolution of secondary alcohols (*rac-2a-c*) in batch (A) and in continuous-flow mode (B)

## 2. Results and Discussion

For this study, three indole-substituted cyclohexanols (*rac-2a-c*) were synthesised by a slight modification of the process described for the preparation of *rac-2a* (Scheme 1)<sup>67</sup> i.e. the ring opening of cyclohexene oxide with the corresponding indole derivative (**1a-c**) using NaH (1 equiv.) in dry DMF. The indoles (**1b** and **1c**) bearing slightly electron donating substituents showed similar reactivity as the unsubstituted indole (**1a**) providing the new indole-substituted *trans*-cyclohexanols (*rac-2b* and *rac-2c*) in excellent yields.

### 2.1. Kinetic resolution of secondary alcohols (*rac-2a-c*) in batch mode

KRs of the indole-substituted secondary alcohols (*rac*-**2a–c**) were carried out with 23 different lipases by acylation with vinyl acetate (Table 1).

**Table 1.** Lipase-catalysed kinetic resolution of secondary alcohols (*rac*-**2a–c**) by acylation with vinyl acetate in batch mode (30°C, shake flask).

Entry	Substrate	Enzyme	<i>c</i> (%) <sup>a</sup>	<i>ee</i> <sub>(<i>R,R</i>)-<b>3a–c</b></sub> (%) <sup>b</sup>	<i>E</i> <sup>c</sup>	<i>r</i> <sub>batch</sub> (μmol g <sup>-1</sup> h <sup>-1</sup> )
Panel A <sup>d</sup>						
1	<i>rac</i> - <b>2a</b>	CaLB N435	49.9	>99.9	»200	32.6
2	<i>rac</i> - <b>2a</b>	Lipobond PS	47.2	>99.9	»200	30.8
3	<i>rac</i> - <b>2a</b>	Lipozyme TLIM	40.2	>99.9	»200	26.2
4	<i>rac</i> - <b>2a</b>	Lipozyme MmL	38.7	>99.9	»200	25.3
5	<i>rac</i> - <b>2a</b>	Amano AK	37.0	>99.9	»200	24.1
6	<i>rac</i> - <b>2a</b>	CaLA G250P	25.1	99.8	»200	16.4
7	<i>rac</i> - <b>2a</b>	CaLA T2-150	14.7	99.6	»200	9.6
8	<i>rac</i> - <b>2a</b>	MpL G250P	13.9	99.9	»200	9.0
9	<i>rac</i> - <b>2a</b>	MpL G250O	11.1	99.9	»200	7.2
10	<i>rac</i> - <b>2a</b>	CaLB G250P	9.4	99.9	»200	6.2
11	<i>rac</i> - <b>2a</b>	PaL G250P	8.6	99.8	»200	5.6
Panel B <sup>e</sup>						
12	<i>rac</i> - <b>2b</b>	CaLB N435	41.2	>99.9	»200	37.6
13	<i>rac</i> - <b>2b</b>	Lipobond PS	27.7	>99.9	»200	25.0
14	<i>rac</i> - <b>2b</b>	Lipozyme TLIM	27.4	>99.9	»200	25.0
15	<i>rac</i> - <b>2b</b>	Lipozyme MmL	24.1	>99.9	»200	21.7
16	<i>rac</i> - <b>2b</b>	CaLB G250P	12.9	99.9	»200	11.9
17	<i>rac</i> - <b>2b</b>	Amano AK	9.0	99.9	»200	8.1
18	<i>rac</i> - <b>2b</b>	Amano M	6.5	99.9	»200	5.9
19	<i>rac</i> - <b>2b</b>	Amano PS	5.5	99.8	»200	5.0
Panel C <sup>e</sup>						
20	<i>rac</i> - <b>2c</b>	Lipozyme TLIM	44.9	>99.9	»200	38.6
21	<i>rac</i> - <b>2c</b>	CaLB N435	38.7	>99.9	»200	33.0
22	<i>rac</i> - <b>2c</b>	Lipozyme MmL	34.4	>99.9	»200	29.1
23	<i>rac</i> - <b>2c</b>	Lipobond PS	33.5	>99.9	»200	28.5
24	<i>rac</i> - <b>2c</b>	Amano AK	27.0	99.9	»200	22.8
25	<i>rac</i> - <b>2c</b>	CaLB G250P	13.7	99.9	»200	11.7
26	<i>rac</i> - <b>2c</b>	CaLA G250P	10.6	99.9	»200	9.0
27	<i>rac</i> - <b>2c</b>	CrL	7.3	99.9	»200	6.2
28	<i>rac</i> - <b>2c</b>	Amano PS	7.2	99.8	»200	6.1
29	<i>rac</i> - <b>2c</b>	CaLA T2-150	6.9	99.8	»200	5.9

<sup>a</sup> Results are shown only for reactions with *c* >5%.

<sup>b</sup> Enantiomeric excess of ester (*ee*<sub>(*R,R*)-**3a–c**</sub>) was determined by chiral GC.

<sup>c</sup> Enantiomeric ratio (*E*) was calculated from *c* and *ee*<sub>(*R,R*)-**3a–c**</sub>.<sup>68</sup> For simplicity, *E* values calculated above 500 were given as »200.

<sup>d</sup> Reaction time 72 h.

<sup>e</sup> Reaction time 48 h.

The KRs were performed in hexane–*tert*-butyl methyl ether (2:1) at 30°C using various forms of the lipases (such as lyophilised powder, adsorbed on surface-modified silica gel,

acrylic or ion-exchange resins, as well as covalently attached to acrylic resin). In the KR of the unsubstituted indole derivative *rac-2a*, excellent enantiomer selectivity ( $E \gg 200$ ) was observed with most of the biocatalysts (Table 1, Panel A). Enantiomeric excess of the product (*R,R*)-**3a** was predominantly at least 99.9%. Moreover, this could be realised at conversions of 35% or above with five lipase preparations while KR was almost complete (nearly 50% conversion) with CaLB N435 or Lipobond PS. Although in the case of CaLA or CaLB significant differences were found in selectivity and activity due to the nature of the hydrophobic grafting of the silica gel supports,<sup>69</sup> in the case of MpL no significant differences were observed between the forms adsorbed onto phenyl- and octyl-grafted silica gels (Entries 8 and 9, respectively).

In the case of several other lipases, however, remarkable variations were found when the same lipase was immobilised by different methods. Such phenomena were observed when CaLA was adsorbed either on phenyl-grafted silica gel or attached covalently to porous polymethacrylate beads (Entries 6 and 7, respectively) or when CaLB was adsorbed on acrylic resin or on phenyl modified silica gel (Entries 1 and 10, respectively). In the case of CaLA, the phenyl silica-adsorbed form showed both higher activity and selectivity (Entry 6) than the other form (Entry 7). The high enantiomer selectivity of CaLA with *rac-2a* ( $E \gg 200$ ) is also noteworthy, because in other KRs of various secondary alcohols this lipase was not particularly selective.<sup>36,69,70</sup> With CaLB, adsorbed on acrylic resin (Entry 1) was much more active but similarly selective than when adsorbed onto phenyl silica (Entry 10). Surprisingly, the lipase from *Burkholderia cepacia* exhibited no activity as lyophilised powder (Amano PS) or when adsorbed on octyl-grafted silica gel (data not shown in Table 1), whereas excellent enantiomeric excess values and conversions were observed when it was covalently attached to acrylic resin (Entry 2).

The KRs of *rac-2b* (Table 1, Panel B) proceeded quite similarly to those of *rac-2a*. The best selectivity and activity was achieved with the same four biocatalysts (CaLB N435, Lipobond PS, Lipozyme TLIM and Lipozyme MmL; Entries 12–15) as with of *rac-2a*. Although, each biocatalysts showed somewhat lower activity compared to the series with *rac-2a*, excellent enantiomer selectivity was maintained ( $E \gg 200$ ; Entries 12–15).

Amano AK proved to be much less active with *rac-2b* ( $c=9.0\%$  in Entry 5) than with *rac-2a* ( $c=37.0\%$  in Entry 17), but its high selectivity ( $E \gg 200$  and  $ee_{(R,R)\text{-}3a} \geq 99.9\%$ ) was retained. Surprisingly, CaLA and MpL which were active on *rac-2a* (Entries 6–9) did not exhibit any notable activity on *rac-2b*. On the other hand, the lyophilised lipases Amano M and Amano PS which were apparently inactive with *rac-2a* catalysed the acylation of *rac-2b* (Entries 18

and 19). These results indicated that a substituent of moderate size at position 3 of the indole moiety in **2b** did not cause much variation among the various lipases concerning the relative binding orientation of the enantiomers of **2b** as compared to those of **2a** but influenced only their binding ability.

The KR results with *rac-2c* are shown in Table 1 (Panel C). The fact that Lipozyme TLIM was significantly more active (Entry 20) than CaLB N435 (Entry 21) indicated that 5-MeO-substitution of the indole moiety requires a quite different steric environment within the active site than the one necessary for the two previously discussed 2-(1-indolyl)cyclohexanols (*rac-2a-b*). In the case of CrL, the different steric requirement for efficient catalysis in the KR of *rac-2c* was also obvious, because this lipase was active only in the KR of the 5-MeO-substituted substrate. It showed moderate activity and excellent enantiomer selectivity (Entry 27) but was apparently inactive with the other two cyclohexanols (*rac-2a-b*). Although CaLB was not the most active biocatalyst in KR of *rac-2c*, but demonstrated a high degree of enantiomer selectivity (Entries 21 and 25). This applied to both forms of CaLA in KR of *rac-2c* (Entries 26 and 29). Similarly, excellent selectivities could be achieved with Lipozyme MmL, Lipobond PS, Amano AK and Amano PS at lower conversions (Entries 22, 23, 24 and 28, respectively).

## 2.2. Continuous-flow kinetic resolution of secondary alcohols (*rac-2a-c*)

KRs in continuous-flow mode were carried out in a multicolumn reactor system (Figure 1) assembled within a multicolumn metal block reactor (Figure 1B), an external cooling-heating thermostat, a temperature control unit and an isocratic HPLC pump. The reactions in continuous-flow mode (Figure 1C) were performed in stainless steel packed bed CatCart<sup>TM</sup> columns filled with the proper biocatalyst.

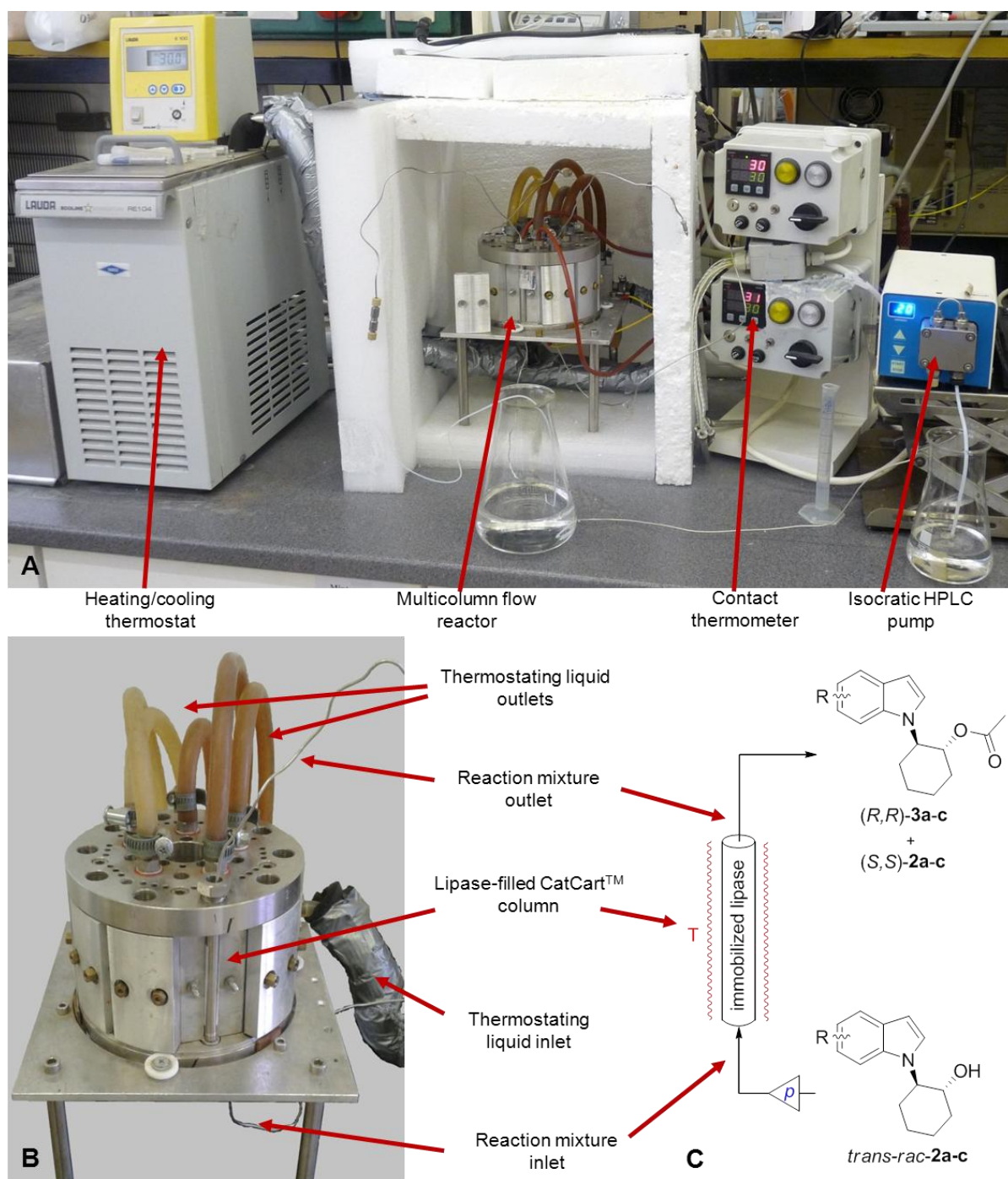


**Figure 1.** A multicolmn continuous-flow reactor system (A). The multicolmn reactor block (B) and the scheme of the KR in the continuous-flow reactor (C: *rac-2a-c*) are also shown.

Selection of biocatalysts to study the KR of *rac-2a-c* in continuous-flow mode was based on the results of KR of *rac-2a-c* in batch experiments. Thus, continuous-flow KR were investigated using Amano AK, CaLA Dv250P, CaLB N435, Lipobond PS, Lipozyme MmL and Lipozyme TLIM for *rac-2a*, further CaLB N435, Lipobond PS, Lipozyme MmL and Lipozyme TLIM for *rac-2b* and *rac-2c*. A solution of *rac-2a-c* and vinyl acetate in hexane-*tert*-butyl methyl ether (2:1) was pumped through the lipase filled column thermostated to a



certain temperature (10°C steps in the 0°C to 60°C or 0°C to 70°C range) at a flow rate of 0.2 mL/min. Samples were taken when reaching the stationary state (30 min after starting a new run) and analysed by GC (Section 4.2.).

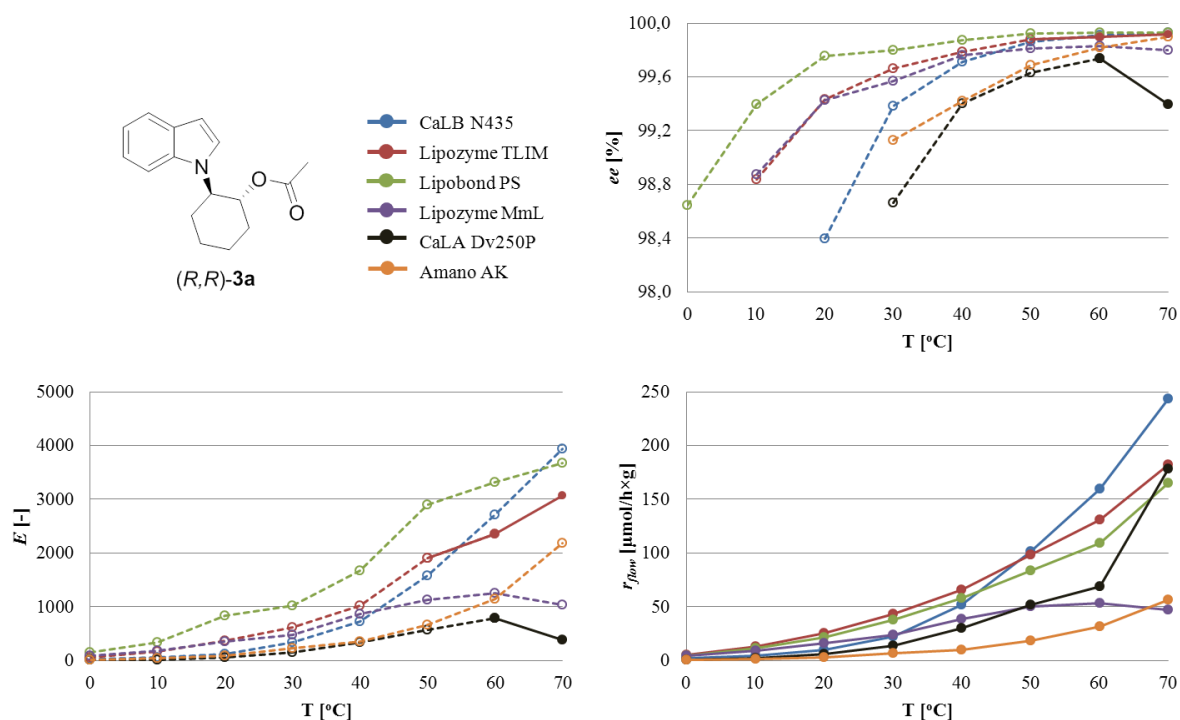


**Figure 2.** Temperature dependent biocatalytic properties ( $E$ ,  $ee$  and  $r_{flow}$ ) of various lipase biocatalysts in the kinetic resolution of *rac*-2a by acylation with vinyl acetate in a continuous-flow reactor. Unfilled markers and dashed lines are from GC measurements with the minor enantiomers under detection limits; see Section 4.2.

The results of KR of *rac*-2a in continuous-flow mode are shown in Figure 2. In accordance with the KR in batch mode, the different biocatalysts exhibited diverse productivity (specific reaction rate,  $r_{flow}$ ) but less variable and high enantiomer selectivity ( $E$  values from  $>100$  to  $\gg 200$ , between 20 and 60°C). All active biocatalysts behaved similarly and their productivity increased exponentially between 0 and 70°C, except for Lipozyme MmL (where  $r_{flow}$  stopped increasing at around 50°C). This indicated the thermostability of all investigated lipases, except of Lipozyme MmL up to 70°C under the investigated continuous-flow conditions. Lipozyme TLIM showed the highest productivity (0–40°C) while Amano AK was the least active in KR of *rac*-2a in continuous-flow mode. Lipobond PS was the most selective biocatalyst in the ambient temperature regime between 20 and 50°C ( $E \gg 200$  and  $ee_{(R,R)\text{-}3a}$  from 99.8 to  $>99.9\%$ ) and even at high temperature such as 70°C ( $E \gg 200$  and  $ee_{(R,R)\text{-}3a} >99.9\%$ ). Although CaLB N435 did not show notable productivity in the lower temperature range (below 20°C), its productivity increased drastically from 30°C and it was the most active catalyst above 50°C. Importantly, it exhibited also excellent selectivity at 70°C ( $E \gg 200$  and  $ee_{(R,R)\text{-}3a} >99.9\%$ ). CaLA Dv250P behaved differently than the other biocatalysts. In a

wide range of temperature (0–60°C) its productivity ( $r_{flow}$ ) increased only moderately but  $r_{flow}$  almost tripled when the temperature rose from 60°C to 70°C. CaLA Dv250P was the only catalyst with significant drop in selectivity at high temperature:  $ee_{(R,R)\text{-}3a}$  dropped from 99.7% at 60°C to 99.4% at 70°C.

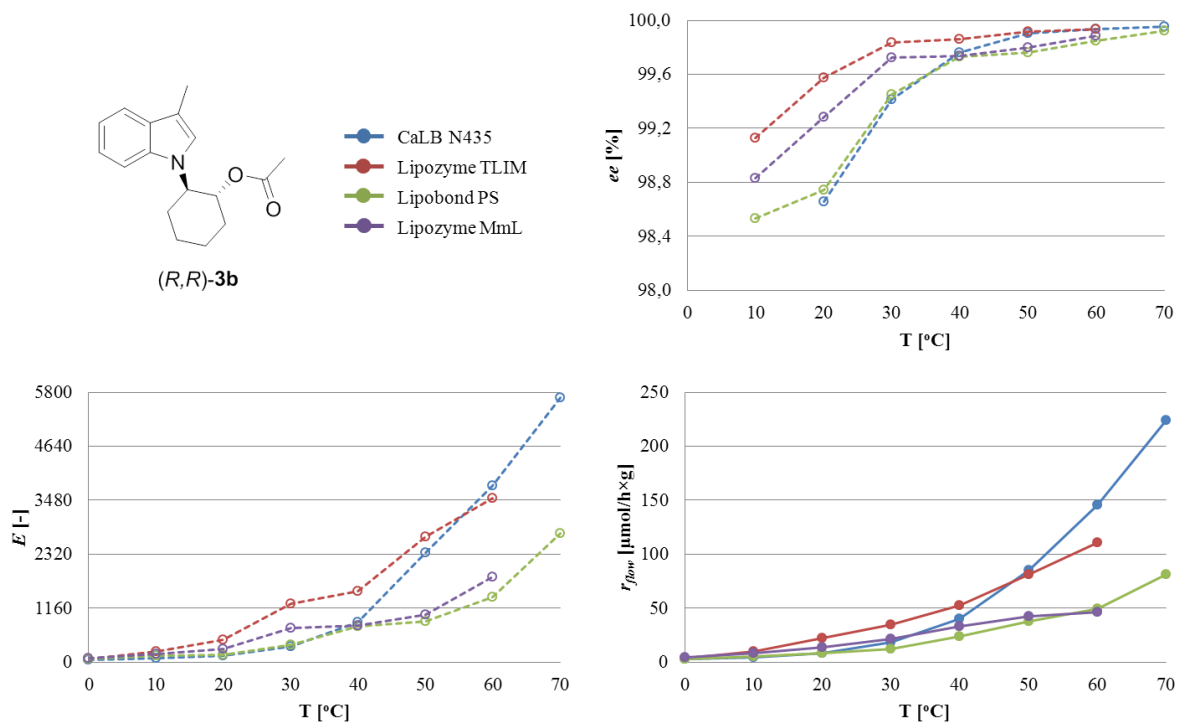


**Figure 3.** Temperature dependent biocatalytic properties ( $E$ ,  $ee$  and  $r_{flow}$ ) of various lipase biocatalysts in kinetic resolution of  $rac\text{-}2b$  by acylation with vinyl acetate in a continuous-flow reactor. Unfilled markers and dashed lines are from GC measurements with the minor enantiomers under detection limits; see Section 4.2.

Those four lipases (CaLB N435, Lipobond PS, Lipozyme TLIM and Lipozyme MmL) which showed the highest activities in batch mode KRs of the 3-methyl-substituted-indole substrate ( $rac\text{-}2b$ , Entries 12–15 in Table 1) were further studied at various temperatures in the continuous-flow mode KRs of  $rac\text{-}2b$  (Figure 3). Investigations of the two most active ones (CaLB N435 and Lipobond PS) between 0–70°C and the further two (Lipozyme TLIM and Lipozyme MmL) between 0–60°C (Figure 3) showed quite similar temperature-dependent biocatalytic behaviour to those found in the KRs of  $rac\text{-}2a$  (Figure 2). At the low temperature range (0–20°C) CaLB N435 was almost inactive in the KR of  $rac\text{-}2b$ , while in the range of 20–70°C exponential ascend of  $r_{flow}$  was observed. CaLB N435 and Lipozyme TLIM were the most selective lipases in the KR of  $rac\text{-}2b$  above 50°C ( $E \gg 200$  and  $ee_{(R,R)\text{-}3b} > 99.9\%$ ). Lipobond PS exhibited lower but still exponentially increasing productivity from 0°C to 70°C with excellent selectivity at high temperature ( $E \gg 200$  and  $ee_{(R,R)\text{-}3b} > 99.9\%$  at 70°C). Thermostability of Lipozyme MmL proved to be poor in the continuous-flow KR of  $rac\text{-}2b$  as well, because  $r_{flow}$  did not increase above 50°C.

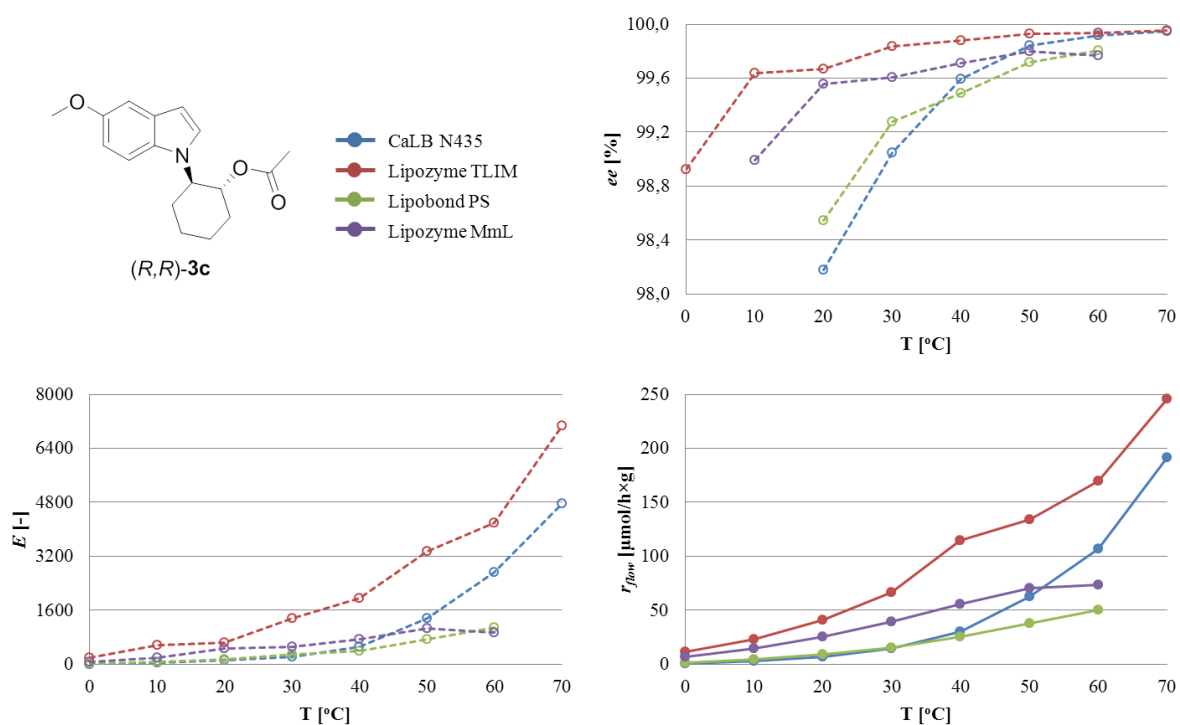


**Figure 4.** Temperature dependent biocatalytic properties ( $E$ ,  $ee$  and  $r_{flow}$ ) of various lipase biocatalysts in kinetic resolution of *rac*-**2c** by acylation with vinyl acetate in a continuous-flow reactor. Unfilled markers and dashed lines are from GC measurements with the minor enantiomers under detection limits; see Section 4.2.

Again, the four lipases (CaLB N435, Lipobond PS, Lipozyme TLIM and Lipozyme MmL) showing the highest activity in batch mode KRs of the 5-methoxy-substituted-indole substrate (*rac*-**2c**, Entries 20–23 in Table 1) were studied at various temperatures in the continuous-flow mode KRs as well (Figure 4). In this case, the two most active biocatalysts (Lipozyme TLIM and CaLB N435) were studied between 0–70°C and the further two (Lipobond PS and Lipozyme MmL) only between 0–60°C (Figure 3). In accordance with the results in batch mode KRs (Table 1, Panel C) the highest productivity in the whole temperature range (0–70°C) was achieved with Lipozyme TLIM combined with excellent selectivity [ $E \gg 200$  and monotonically increasing  $ee_{(R,R)\text{-}3c}$  from 99.6% (10°C) to  $>99.9\%$  (70°C)]. Contrarily to the KRs of *rac*-**2a** or *rac*-**2b**, where CaLB N435 was the most active biocatalyst in the high temperature range of 50–70°C, its productivity remained lower than that of Lipozyme TLIM in the KRs of *rac*-**2b** at any temperature covered. Although Lipozyme MmL showed good enantiomer selectivity in the ambient temperature range ( $E$  from  $>200$  to  $\gg 200$  and  $ee_{(R,R)\text{-}3c}$  from 99.6% to 99.8% between 20–60°C), its applicability is limited due to the partial deactivation of the enzyme above 50°C. In contrast to the KRs of *rac*-**2a**, the lowest productivity was obtained with Lipobond PS although selectivity with good above 50°C ( $E \gg 200$  and  $ee_{(R,R)\text{-}3c} >99.7\%$ ).

In conclusion, generally higher productivity can be obtained at the high temperature range (50–70°C) with all the investigated biocatalysts but Lipozyme MmL. Enantiomeric selectivity of the lipase-catalysed KRs of *rac*-**2a–c** did not drop with increasing temperature due to the fact that *trans*-1-(2-hydroxycyclohexyl)-indoles (*rac*-**2a–c**) are rather bulky and conformationally rigid substrates.

### 2.3. Preparation of enantiomerically enriched alcohols (**2a–c**) and acetates (**3a–c**) in flow mode at preparative scale

The crucial issue in the development of a preparative scale method is finding the optimal temperature at which productivity, selectivity and lifetime of the enzyme are balanced. In general, productivity is increasing with increasing temperature, although at higher temperature lifetime of the biocatalyst may suffer decrease. Since the best overall performance in the continuous-flow KR of all the three substrates (*rac*-**2a–c**) could be achieved with CaLB N435 in the high temperature range ( $r_{flow} > 100 \mu\text{mol}/(\text{h}\times\text{g})$ ,  $E \gg 200$  and  $ee_{(R,R)\text{-3a-c}} > 99.9\%$  at and above 60°C), CaLB N435 was selected as biocatalyst to perform flow mode KR at preparative scale. The temperature was chosen to be 50–60°C where CaLB N435 has proved to be both productive and selective without the danger of losing its activity.

For all the three substrates (*rac*-**2a–c**) the same series of six CaLB N435-filled columns was used. Between the runs with different substrates the columns were washed briefly with hexane–*tert*-butyl methyl ether (2:1) with about ten times the dead volume of the bioreactor to remove substrate residues. After 24 h of continuous-flow operation at 50°C, the bioreactor was switched to recirculation-flow mode at 60°C until the conversion reached nearly 50% or the  $ee_{(R,R)\text{-3a-c}}$  (monitored by GC) started to decrease. The obtained (*R,R*)-acetates [(*R,R*)-**3a–c**] and (*S,S*)-alcohols [(*S,S*)-**2a–c**] were separated by column chromatography and the acetates [(*R,R*)-**3a–c**] were deacylated by Zemplén deacylation to yield the (*R,R*)-alcohols [(*R,R*)-**2a–c**] (Table 2). In most of the cases, high enantiomeric excesses values were observed; (*R,R*)-**3a–c**,  $> 99.0\%$ ; (*R,R*)-**2a–c**,  $> 97\text{--}98\%$  and (*S,S*)-**2b–c**,  $> 93\text{--}94\%$ . Only with (*S,S*)-**2a** was  $ee_{(R,R)\text{-2a}} < 90.0\%$ .

**Table 2.** Alcohols prepared by kinetic resolution of *rac*-**2a–c** with vinyl acetate in a CaLB N435-filled continuous-flow reactor at preparative scale followed by Zemplén deacylation of the formed (*R,R*)-**3a–c**.

Compound	Yield (%)	$ee$ (%) <sup>a</sup>	$[\alpha]_D^{26^\circ\text{C}b}$
( <i>R,R</i> )- <b>2a</b>	36 <sup>c</sup>	97.8	+0.86
( <i>S,S</i> )- <b>2a</b>	39	87.9	−0.75
( <i>R,R</i> )- <b>2b</b>	33 <sup>c</sup>	98.1	+0.17
( <i>S,S</i> )- <b>2b</b>	34	94.8	−0.07
( <i>R,R</i> )- <b>2c</b>	35 <sup>c</sup>	98.7	+0.47
( <i>S,S</i> )- <b>2c</b>	33	93.1	−0.19

( <i>R,R</i> )- <b>3a</b>	45	99.1	+12.7
( <i>R,R</i> )- <b>3b</b>	43	99.5	+10.7
( <i>R,R</i> )- <b>3c</b>	42	99.2	+11.8

<sup>a</sup> Enantiomeric excess was determined by chiral GC (see Section 4.2).

<sup>b</sup> Specific rotations, (*c* 1.0, CH<sub>2</sub>Cl<sub>2</sub>).

<sup>c</sup> Combined yield of kinetic resolution and Zemplén deacylation.

During these runs, the CaLB N435-filled columns were used for more than three weeks in total. After all the continuous- and recirculation-flow runs with the three different substrates (*rac*-**2a–c**), testing of the spent CaLB N435-filled columns by KR of the unsubstituted 2-(1-indolyl)cyclohexanol (*rac*-**2a**), between 30–60°C, indicated no observable change in activity or selectivity compared to the first single column tests (Figure 2).

### 3. Conclusion

Batch and continuous-flow methods were investigated for the first time for the lipase-catalysed kinetic resolution of *trans*-1-(2-hydroxycyclohexyl)-indoles (*rac*-**2a–c**) by acetylation with vinyl acetate. The substrates *rac*-**2a–c** could be obtained conveniently by ring opening of cyclohexene oxide with the corresponding indole (**1a–c**). We studied the influence of temperature effect on productivity and selectivity in the 0–70°C range and found that a number of the thermostable biocatalysts produced higher productivity with excellent enantiomer selectivity in the continuous-flow KR of *rac*-**2a–c** in the high temperature range (50–70°C) than at low temperatures. Based on this observation, highly enantiomerically enriched alcohols (**2a–c**) and acetates (**3a–c**) were produced by flow mode methods at preparative scale by using a CaLB N435 filled reactor operating at 50–60°C.

## 4. Experimental

### 4.1. Materials

All chemicals and starting materials were purchased from Sigma-Aldrich (Saint Louis, MO, USA) and Alfa Aesar Europe (Karlsruhe, Germany) and used without further purification.

Prior to use, solvents from Merck KGaA (Darmstadt, Germany) were dried and/or freshly distilled.

Amano A (lipase from *Aspergillus niger*), Amano AK (lipase from *Pseudomonas fluorescens*), Amano AYS (lipase from *Candida rugosa*), Amano F-AP15 (lipase from *Rhizopus oryzae*), Amano G (lipase from *Penicillium camamberti*), Amano M (lipase from *Mucor javanicus*), Amano PS (lipase from *Burkholderia cepacia*), CrL (lipase from *Candida rugosa*), Lipozyme<sup>®</sup> MmL (Lipozyme MmL, lipase from *Mucor miehei*, immobilized on

macroporous ion-exchange resin), Lipozyme<sup>®</sup> TLIM (Lipozyme TLIM, lipase from *Thermomyces lanuginosus*, immobilized on ion-exchange resin), Novozym<sup>®</sup> 435 (CaLB N435, lipase B from *Candida antarctica*, adsorbed on acrylic resin) and PPL (lipase from porcine pancreas) were purchased from Sigma Aldrich (Saint Louis, MO, USA). CaLA T2-150 (lipase A from *Candida antarctica*, covalently attached to dry acrylic beads of 150-300  $\mu\text{m}$  particle size) and CaLB T2-150 (lipase B from *Candida antarctica*, covalently attached to dry acrylic beads of 150-300  $\mu\text{m}$  particle size) were the products of ChiralVision BV (Leiden, The Netherlands). Lipobond PS (lipase from *Burkholderia cepacia*, covalently immobilized on a highly hydrophobic support) was obtained from Iris Biotech GmbH (Marktredwitz, Germany). AK Dv250P (lipase from *Pseudomonas fluorescens*, adsorbed on phenyl-functionalized silica gel), CaLA Dv250P (lipase from *Candida antarctica*, adsorbed on phenyl-functionalized silica gel), CaLB Dv250P (lipase from *Candida antarctica*, adsorbed on phenyl-functionalized silica gel), CrL Dv250O (lipase from *Candida rugosa*, adsorbed on octyl-functionalized silica gel), MpL Dv250O (lipase from *Malbranchea pulchella*, adsorbed on octyl-functionalized silica gel), MpL Dv250P (lipase from *Malbranchea pulchella*, adsorbed on phenyl-functionalised silica gel), PaL Dv250P (lipase from *Pseudozyma aphidis*, adsorbed on phenyl-functionalised silica gel) and PS Dv250O (lipase from *Burkholderia cepacia*, adsorbed on octyl-functionalized silica gel) were the products of SynBiotec Ltd. (Budapest, Hungary).

## 4.2. Methods

TLC was carried out using Kieselgel 60 F<sub>254</sub> (Merck) sheets. Spots were visualized under UV light (254 nm and 365 nm) or by treatment with 5% ethanolic phosphomolybdic acid solution and heating of the dried plates. Optical rotations were taken on a Perkin-Elmer 241 polarimeter that was calibrated by measuring the optical rotations of both enantiomers of menthol. The NMR spectra were recorded in CDCl<sub>3</sub> on a Bruker DRX-300 spectrometer operating at 300 MHz for <sup>1</sup>H and 75 MHz for <sup>13</sup>C, and signals are given in ppm on the  $\delta$  scale. Infrared spectra were recorded on a Bruker ALPHA FT-IR spectrometer and wavenumbers of bands are listed in cm<sup>-1</sup>.

Reactions were analysed by GC on an Agilent 5890 equipment using Hydrodex  $\beta$ -TBDAC column (Machery-Nagel; 25 m  $\times$  0.25 mm  $\times$  0.25  $\mu\text{m}$ , heptakis-(2,3-di-*O*-acetyl-6-*O*-*t*-butyldimethylsilyl)- $\beta$ -cyclodextrin) [FID (250°C), injector (250°C), H<sub>2</sub> (12 psi, split ratio: 1:50)]. GC data [(oven program);  $t_r$  (min)]: for **2a** and **3a** [(100–190°C, 9°C/min, 15 min at 190°C), (*S,S*)-**3a**: 18.9, (*R,R*)-**3a**: 19.4, (*S,S*)-**2a**: 21.1, (*R,R*)-**2a**: 21.6]; for **2b** and **3b** [(100–190°C,

9°C/min, 20 min at 190°C); (*S,S*)-**3b**: 20.9, (*R,R*)-**3b**: 21.4, (*S,S*)-**2a**: 24.9, (*R,R*)-**2a**: 25.5]; for **2c** and **3c** [(45 min at 190°C); (*S,S*)-**3c**: 30.9, (*R,R*)-**3c**: 32.0, (*S,S*)-**2c**: 37.2, (*R,R*)-**2c**: 38.2]. In Figures 2–4, data points are shown only for cases with *ee* >98.0%. The solid curves and filled markers indicate data which arose from a precise integration of chromatograms in which both enantiomers of the products **3a–c** were clearly visible. When signals for the minor enantiomer [(*S,S*)-**3a–c**] were indistinguishable from noise, the dashed lines and unfilled markers indicate values which are possible minimum values of *ee* and *E*.

Conversion (*c*), enantiomeric excess (*ee*) and enantiomeric ratio (*E*) were determined by GC. Enantiomeric ratio (*E*) was calculated from *c* and enantiomeric excess of the product (*ee<sub>p</sub>*) using the equation  $E = \ln[1 - c(1+ee_p)]/\ln[1 - c(1 - ee_p)]$ .<sup>68</sup> For simplicity, *E* values calculated in the range of 100–200 were given as >100, those in the range of 200–500 as >200 and above 500 as »200. To characterize the productivity of the biocatalysts, specific reaction rates in batch reactions (*r<sub>batch</sub>*) were calculated using the equation  $r_{\text{batch}} = n_p/(t \times m_B)$  (where *n<sub>p</sub>* [μmol] is the amount of the product, *t* [h] is the reaction time and *m<sub>B</sub>* [g] is the mass of the applied biocatalyst).<sup>65</sup> Specific reaction rates in continuous-flow systems (*r<sub>flow</sub>*) were calculated using the equation  $r_{\text{flow}} = [P] \times v/m_B$  (where [*P*] [μmol/mL] is the molar concentration of the product, *v* [mL/h] is the flow rate and *m<sub>B</sub>* [g] is the mass of the applied biocatalyst).<sup>65</sup> Because the rate of product formation is not a linear function of *c*, rigorous comparisons between the productivity of a continuous-flow reaction and its batch mode counterpart using their *r* values can only be made at comparable degrees of conversions.<sup>65</sup>

Continuous-flow kinetic resolutions were performed in a laboratory flow reactor comprising an isocratic HPLC pump (Knauer K-120) attached to stainless steel columns (ThalesNano CatCart™) filled with the immobilized lipase biocatalysts in an in-house made thermostated aluminium metal block multicolumn holder with precise temperature control (Figure 1). Before use, the lipase-filled columns were washed with a 2:1 mixture of hexane and *tert*-butyl methyl ether (0.5 mL/min, 20 min).

Enzymes were filled into stainless steel CatCart™ columns according to the process of ThalesNano Inc. For the continuous-flow enzymatic applications both ends of the columns were sealed with PTFE sealings and silver metal filter membranes (Sterlitech Silver Membrane Filter from Sigma–Aldrich, Z623237, pore size 0.45 μm; pure metallic silver, 99.97% with no extractable or detectable contaminants).

### 4.3. Synthesis of racemic secondary alcohols (*rac-2a-c*)

Secondary alcohols were obtained by a slightly modified method of Gharpure, J. S. and Sathiyarayanan, A. M.<sup>67</sup> A solution of the indole (**1a**: 0.854 mol, **1b**: 0.381 mol, **1c**: 0.340 mol) in dry DMF (40 mL) was added dropwise to a stirred suspension of NaH (1 equiv.) in dry DMF (60 mL) at 0°C over 15 min. After stirring at 0°C for 20 min, cyclohexene oxide (1 equiv.) was added and the resulting slurry was allowed to warm to room temperature and stirred overnight. Then the reaction mixture was stirred under reflux. When the reaction was completed (monitored by TLC, eluent: CH<sub>2</sub>Cl<sub>2</sub>), it was cooled, quenched by water (50 mL) and extracted with diethyl ether (3×50 mL). The combined organic phases were washed with brine (2×50 mL), dried over Na<sub>2</sub>SO<sub>4</sub> and the solvent was removed under vacuum. The residue was further purified by column chromatography on silica gel eluted with CH<sub>2</sub>Cl<sub>2</sub>.

*rac-2a*: 17.82 g (97%), pale yellow crystals, mp: 85.2–86.0°C, IR (KBr, cm<sup>-1</sup>):  $\nu$  3238, 3098, 2929, 2848, 1717, 1507, 1461, 1311, 1215, 1090, 739; <sup>1</sup>H NMR: 1.38–1.57 (2H, m, CH<sub>2</sub>), 1.76–1.93 (4H, m, CH<sub>2</sub>), 2.03–2.10 (1H, m, CH<sub>2</sub>), 2.17–2.24 (1H, m, CH<sub>2</sub>), 3.88 (1H, td,  $J=9.80$  and 4.14 Hz, O-CH), 4.11 (1H, td,  $J=9.23$  and 3.96 Hz, N-CH), 5.32 (1H, s, OH), 6.60 (1H, d,  $J=2.83$  Hz, CH), 7.11–7.28 (3H, m, CH), 7.50 (1H, d,  $J=8.29$  Hz, CH), 7.66 (1H, d,  $J=7.24$  Hz, CH); <sup>13</sup>C NMR: 24.55 (CH<sub>2</sub>), 25.66 (CH<sub>2</sub>), 32.02 (CH<sub>2</sub>), 33.82 (CH<sub>2</sub>), 62.19 (CH), 73.89 (CH), 102.63 (CH), 110.07 (CH), 119.83 (CH), 121.19 (CH), 121.83 (CH), 124.18 (CH), 128.67 (C), 136.98 (C).

*rac-2b*: 8.08 g (92%), pale yellow crystals, mp: 91.1–92.9°C, IR (KBr, cm<sup>-1</sup>):  $\nu$  3293, 2929, 2851, 1755, 1612, 1553, 1464, 1357, 1224, 1204, 1086, 1015, 943, 735; <sup>1</sup>H NMR: 1.39–1.55 (2H, m, CH<sub>2</sub>), 1.65–1.92 (4H, m, CH<sub>2</sub>), 2.00–2.08 (1H, m, CH<sub>2</sub>), 2.16–2.25 (1H, m, CH<sub>2</sub>), 2.34 (3H, s, CH<sub>3</sub>), 3.80–3.92 (1H, m, O-CH), 3.99–4.10 (1H, m, N-CH), 5.30 (1H, s, OH), 6.99 (1H, s, CH), 7.08–7.16 (1H, m, CH), 7.17–7.25 (1H, m, CH), 7.43 (1H, d,  $J=8.23$  Hz, CH), 7.58 (1H, d,  $J=7.91$  Hz, CH); <sup>13</sup>C NMR: 9.94 (CH<sub>3</sub>), 24.60 (CH<sub>2</sub>), 25.73 (CH<sub>2</sub>), 32.06 (CH<sub>2</sub>), 33.76 (CH<sub>2</sub>), 61.97 (CH), 73.93 (CH), 109.83 (C), 111.92 (CH), 119.17 (CH), 119.28 (CH), 121.72 (CH), 121.85 (CH), 128.91 (C), 137.34 (C).

*rac-2c*: 8.18 g (98%), yellow oil, IR (film, cm<sup>-1</sup>):  $\nu$  3270, 2933, 2856, 1620, 1479, 1448, 1233, 1151, 1067, 1030, 948, 792, 712; <sup>1</sup>H NMR: 1.37–1.52 (2H, m, CH<sub>2</sub>), 1.73–1.91 (4H, m, CH<sub>2</sub>), 2.05 (1H, m, CH<sub>2</sub>), 2.19 (1H, m, CH<sub>2</sub>), 3.82–3.89 (4H, m, O-CH<sub>3</sub> and O-CH), 3.97–4.07 (1H, m, N-CH), 5.31 (1H, s, OH), 6.46–6.54 (1H, m, CH), 6.86–6.93 (1H, m, CH), 7.08–7.13 (1H, m, CH), 7.15–7.20 (1H, m, CH), 7.36 (1H, d,  $J=8.85$  Hz, CH); <sup>13</sup>C NMR: 24.55 (CH<sub>2</sub>), 25.67 (CH<sub>2</sub>), 32.02 (CH<sub>2</sub>), 33.81 (CH<sub>2</sub>), 56.08 (CH<sub>3</sub>), 62.44 (CH), 73.98 (CH), 102.18



(CH), 102.72 (CH), 110.81 (CH), 112.24 (CH), 124.77 (CH), 128.97 (C), 132.26 (C), 154.33 (C).

#### 4.4. Synthesis of racemic acetates (*rac-3a-c*)

To a mixture of the corresponding alcohol (**2a**: 1.39 mmol, **2b**: 1.31 mmol, **2c**: 1.22 mmol) in acetic anhydride (2 mL), catalytic amount (1 drop) of cc. H<sub>2</sub>SO<sub>4</sub> was added at room temperature and the resulting slurry was stirred for 1 min (the reaction completed by TLC). After adding hexane (5 mL) to the mixture, it was washed with 10% Na<sub>2</sub>CO<sub>3</sub> (3×5 mL) and brine (5 mL), the organic phase was dried over Na<sub>2</sub>SO<sub>4</sub> and the solvent was removed under vacuum. No further purification was necessary.

*rac-3a*: 83 mg (23%), white crystals, mp: 63.3–65.2°C, IR (KBr, cm<sup>-1</sup>):  $\nu$  3045, 2939, 2860, 1748, 1607, 1510, 1475, 1460, 1373, 1314, 1229, 1034, 745; <sup>1</sup>H NMR: 1.41–1.67 (3H, m, CH<sub>2</sub>), 1.81–2.03 (3H, m, CH<sub>2</sub>), 2.11–2.27 (2H, m, CH<sub>2</sub>), 4.26–4.36 (1H, m, N-CH), 5.07–5.21 (1H, m, O-CH), 6.54–6.56 (1H, m, CH), 7.05–7.15 (1H, m, CH), 7.17–7.30 (2H, m, CH), 7.44 (1H, d,  $J=8.28$  Hz, CH), 7.62 (1H, d,  $J=7.89$  Hz, CH); <sup>13</sup>C NMR: 20.47 (CH<sub>3</sub>), 24.41 (CH<sub>2</sub>), 25.40 (CH<sub>2</sub>), 31.97 (CH<sub>2</sub>), 32.15 (CH<sub>2</sub>), 58.23 (CH), 75.04 (CH), 102.31 (CH), 109.83 (CH), 119.47 (CH), 121.08 (CH), 121.37 (CH), 124.14 (CH), 128.50 (C), 136.94 (C), 170.08 (CO).

*rac-3b*: 101 mg (28%), brown crystals, mp: 78.4–80.1°C, IR (KBr, cm<sup>-1</sup>):  $\nu$  3061, 2939, 2861, 1739, 1613, 1463, 1452, 1359, 1297, 1235, 1125, 1031, 739; <sup>1</sup>H NMR: 1.43–1.60 (3H, m, CH<sub>2</sub>, CH<sub>3</sub>), 1.78–1.95 (3H, m, CH<sub>2</sub>), 2.07–2.22 (2H, m, CH<sub>2</sub>), 2.30 (3H, s, CH<sub>3</sub>), 4.18–4.28 (1H, m, N-CH), 5.02–5.11 (1H, m, O-CH), 6.94 (1H, s, CH), 7.07 (1H, t,  $J=7.74$  Hz, CH), 7.18 (1H, t,  $J=7.16$  Hz, CH), 7.36 (1H, d,  $J=8.29$  Hz, CH), 7.52 (1H, d,  $J=7.91$  Hz, CH); <sup>13</sup>C NMR: 9.95 (CH<sub>3</sub>), 20.88 (CH<sub>3</sub>), 24.44 (CH<sub>2</sub>), 25.43 (CH<sub>2</sub>), 31.98 (CH<sub>2</sub>), 32.25 (CH<sub>2</sub>), 57.96 (CH), 75.12 (CH), 109.65 (CH), 111.35 (C), 118.74 (CH), 119.06 (CH), 121.30 (CH), 121.64 (CH), 128.74 (C), 137.30 (C), 170.22 (CO).

*rac-3c*: 59 mg (17%), white crystals, mp: 70.3–72.8°C, IR (KBr, cm<sup>-1</sup>):  $\nu$  2997, 2938, 2855, 1732, 1618, 1484, 1453, 1376, 1254, 1233, 1157, 1125, 1033, 796, 717; <sup>1</sup>H NMR: 1.42–1.63 (3H, m, CH<sub>2</sub>), 1.82–1.99 (3H, m, CH<sub>2</sub>), 2.09–2.25 (2H, m, CH<sub>2</sub>), 3.85 (3H, s, CH<sub>3</sub>), 4.14–4.29 (1H, m, N-CH), 5.01–5.16 (1H, m, O-CH), 6.46 (1H, s, CH), 6.87 (1H, d,  $J=9.0$  Hz, CH), 7.07 (1H, s, CH), 7.16 (1H, s, CH), 7.31 (1H, d,  $J=9.0$  Hz, CH); <sup>13</sup>C NMR: 20.65 (CH<sub>3</sub>), 24.24 (CH<sub>3</sub>), 25.23 (CH<sub>2</sub>), 31.77 (CH<sub>2</sub>), 31.96 (CH<sub>2</sub>), 55.85 (CH<sub>2</sub>), 58.29 (CH), 74.99 (CH), 101.69 (CH), 102.33 (C), 110.42 (CH), 111.65 (CH), 124.51 (CH), 128.54 (CH), 132.12 (C), 153.86 (C), 169.91 (CO).

#### 4.5. Enantiomer selective acetylation of racemic alcohols (*rac-2a-c*) in batch mode

To a solution of the alcohol (25 mg, *rac-2a-c*) in hexane-*tert*-butyl methyl ether-vinyl acetate 6:3:1 (2 mL) in an amber screw cap vial, the enzyme (25 mg) was added and the mixture was shaken (1000 rpm) in the closed vial at 30°C for 72 h. Samples (50 µL, diluted with CH<sub>2</sub>Cl<sub>2</sub> to 300 µL) were taken directly from the reaction mixture after 1, 4, 8, 24, 48 and 72 h and analysed by GC as described in Section 4.2.

#### 4.6. Enantiomer selective acetylation of racemic alcohols (*rac-2a-c*) in continuous-flow bioreactors

Separate CatCart<sup>TM</sup> columns were packed for each substrate (*rac-2a-c*) in this study [filling weights: for KRs of *rac-2a* (CaLA Dv250P: 202 mg, CaLB N435: 256 mg, Lipozyme TLIM: 290 mg, Amano AK: 411 mg, Lipobond PS: 307 mg and Lipozyme MmL: 250 mg); for KRs of *rac-2b* (CaLB N435: 237 mg, Lipozyme TLIM: 286 mg, Lipobond PS: 276 mg and Lipozyme MmL: 233 mg); for KRs of *rac-2c* (CaLB N435: 224 mg, Lipozyme TLIM: 301 mg; Lipobond PS: 280 mg and Lipozyme MmL: 245 mg)].

The alcohol (5 mg/mL, *rac-2a-c*) dissolved in a 6:3:1 mixture of hexane-*tert*-butyl methyl ether-vinyl acetate was pumped through the enzyme-packed column thermostated at various temperatures (0–70°C) at a flow rate of 0.2 mL/min. Experiments were run in 10°C steps at temperatures of 0–70°C. Samples were collected after stationary operation has been established (sample size 100 µL, diluted with CH<sub>2</sub>Cl<sub>2</sub> to 250 µL; taken 30 min after setting a new temperature) and analysed by GC as described in Section 4.2. Results for KRs of *rac-2a-c* are shown in Figures 3–5, respectively.

#### 4.7. Kinetic resolution of racemic alcohols (*rac-2a-c*) in continuous-flow bioreactors at preparative scale

A series of six serially-connected CaLB N435-filled CatCart<sup>TM</sup> columns (total filling weight: 1373 mg) was used for the preparative scale kinetic resolutions of the substrates (*rac-2a-c*). Before and after each run, the set of columns was flushed with a 2:1 mixture of hexane-*tert*-butyl methyl ether (0.5 mL/min, 1 h) and the washed columns were stored at 4°C.

The solution of the alcohol (5 mg/mL of *rac-2a-c*) in a 6:3:1 mixture of hexane-*tert*-butyl methyl ether-vinyl acetate was pumped through the enzyme filled column series thermostated to 50°C at a flow rate of 0.15 mL/min. After collecting ~210 mL (24 h) of the reaction mixture the system was switched to recirculation at 60°C until the conversion reached ~45–47%. To check the progress of the reaction, samples were collected (sample size 100 µL, diluted with CH<sub>2</sub>Cl<sub>2</sub> to 250 µL) and analysed by GC as described in Section 4.2.

After finishing the reaction (140–170 h) the solvent was removed under vacuum and the alcohol [(*S,S*)-**2a–c**] and acetate [(*R,R*)-**3a–c**] were separated by column chromatography on silica gel eluted with CH<sub>2</sub>Cl<sub>2</sub>.

(*S,S*)-**2a**: 0.421 g (39%), white crystals, mp: 79.5–81.3°C,  $[\alpha]_D^{26^\circ\text{C}} = -0.75$  (CH<sub>2</sub>Cl<sub>2</sub>), *ee*=87.9% by GC, IR (KBr, cm<sup>-1</sup>):  $\nu$  3427, 3050, 2928, 2856, 1610, 1512, 1463, 1411, 1312, 1251, 1059, 947, 765, 738.

(*S,S*)-**2b**: 0.367 g (34%), white crystals, mp: 74.8–76.1°C,  $[\alpha]_D^{26^\circ\text{C}} = -0.07$  (CH<sub>2</sub>Cl<sub>2</sub>), *ee*=94.8% by GC, IR (KBr, cm<sup>-1</sup>):  $\nu$  3251, 3048, 2930, 2849, 1753, 1613, 1555, 1465, 1385, 1357, 1225, 1206, 1128, 1085, 1015, 942, 805, 736.

(*S,S*)-**2c**: 0.351 g (33%), yellow oil,  $[\alpha]_D^{26^\circ\text{C}} = -0.19$  (CH<sub>2</sub>Cl<sub>2</sub>), *ee*=93.1% by GC, IR (film, cm<sup>-1</sup>):  $\nu$  3412, 2933, 2857, 1720, 1619, 1547, 1480, 1448, 1347, 1234, 1210, 1152, 1067, 1032, 949, 793, 714.

(*R,R*)-**3a**: 0.580 g (45%), pale yellow crystals, mp: 76.1–77.1°C,  $[\alpha]_D^{26^\circ\text{C}} = +12.7$  (CH<sub>2</sub>Cl<sub>2</sub>), *ee*=99.0% by GC, IR (KBr, cm<sup>-1</sup>):  $\nu$  3467, 3055, 2935, 2859, 1923, 1742, 1610, 1556, 1510, 1461, 1409, 1370, 1314, 1230, 1029, 868, 736, 713.

(*R,R*)-**3b**: 0.549 g (43%), white oil,  $[\alpha]_D^{26^\circ\text{C}} = +10.7$  (CH<sub>2</sub>Cl<sub>2</sub>), *ee*=99.5% by GC, IR (film, cm<sup>-1</sup>):  $\nu$  3049, 2937, 2861, 1734, 1612, 1461, 1360, 1297, 1232, 1195, 1033, 909, 736.

(*R,R*)-**3c**: 0.531 g (42%), yellow crystals, mp: 65.1–66.1°C,  $[\alpha]_D^{26^\circ\text{C}} = +11.8$  (CH<sub>2</sub>Cl<sub>2</sub>), *ee*=99.2% by GC, IR (KBr, cm<sup>-1</sup>):  $\nu$  2930, 2860, 1731, 1481, 1450, 1370, 1231, 1155, 1028, 851, 795, 714.

#### 4.8. Zemplén deacetylation of acetates [(*R,R*)-**3a–c**]

To a solution of (*R,R*)-**3a–c** (0.50 g) dissolved in dry methanol (10 mL) 0.1 equiv. of CH<sub>3</sub>ONa was added at 0°C. The resulting solution was stirred at 0°C for 1.5 h then at room temperature until the completion of the reaction (14–18 h, monitored by TLC using CH<sub>2</sub>Cl<sub>2</sub> as eluent). After removing the solvent under vacuum the residue was filtered through a thin layer of silica gel by eluting with a 20:1 mixture of CH<sub>2</sub>Cl<sub>2</sub> and CH<sub>3</sub>OH.

(*R,R*)-**2a**: 0.339 g (81%), pale yellow crystals, mp: 85.9–86.7°C,  $[\alpha]_D^{26^\circ\text{C}} = +0.86$  (CH<sub>2</sub>Cl<sub>2</sub>), *ee*=97.8% by GC, IR (film, cm<sup>-1</sup>):  $\nu$  3387, 2933, 2856, 1508, 1477, 1459, 1410, 1309, 1209, 1065, 948, 869, 735.

(*R,R*)-**2b**: 0.321 g (76%), pale yellow oil,  $[\alpha]_D^{26^\circ\text{C}} = +0.17$  (CH<sub>2</sub>Cl<sub>2</sub>), *ee*=98.1% by GC, IR (film, cm<sup>-1</sup>):  $\nu$  3406, 2932, 2857, 1612, 1460, 1357, 1218, 1191, 1066, 1030, 944, 733.

(*R,R*)-**2c**: 0.359 g (84%), yellow oil,  $[\alpha]_D^{26^\circ\text{C}} = +0.47$  (CH<sub>2</sub>Cl<sub>2</sub>), *ee*=98.7% by GC, IR (film, cm<sup>-1</sup>):  $\nu$  3421, 2933, 2857, 1620, 1479, 1448, 1234, 1151, 1067, 1031, 949, 792, 714.

## Acknowledgements

This project was supported by the New Széchenyi Development Plan ("*Development of quality-oriented and harmonized R+D+I strategy and functional model at BME*" project, TÁMOP-4.2.1/B-09/1/KMR-2010-0002). PF thanks the scholarship from Pro Progressio Foundation (Budapest, Hungary). Thanks are also due to ThalesNano Nanotechnology Inc. for the fillable CatCart™ columns and to Prof. Mihály Nógrádi (Budapest, Hungary) for his valuable comments.

## References

1. Barden T. C. Indoles: Industrial, Agricultural and Over-the-Counter Uses. In *Heterocyclic Scaffolds II (Topics in Heterocyclic Chemistry, Vol 26)*; Gribble, G. W., Ed.; Springer-Verlag, Berlin Heidelberg, **2010**. 31–46.
2. Kaushik, N. K.; Kaushik, N.; Attri, P.; Kumar, N.; Kim, C. H.; Verma, A. K.; Choi, E. H. *Chem. Commun.* **2011**, *47*, 3625–3627.
3. Berger, M; Gray, J. A.; Roth, B. L. *Annu. Rev. Med.* **2009**, *60*, 355–366.
4. Phillipson, O. T. *Neurobiol. Aging.* **2014**, *35*, 847–857.
5. Borroto-Escuela, D. O.; Romero-Fernandez, W.; Narvaez, M.; Oflijan, J.; Agnati, L. F.; Fuxe, K. *Biochem. Biophys. Res. Commun.* **2014**, *443*, 278–284.
6. Chilton, W. S.; Bigwood, J.; Gensen, R. E. *J. Psychedelic Drugs*, **1979**, *11*, 61–69.
7. Jaishree, B.; Manjulatha, K.; Girish, M.; Adil, S.; Purohit, M. G. *Arkivoc*, **2009**, *12*, 217–231.
8. Murphy, J. A.; Scott, K. A.; Sinclair, R. S.; Lewis, N. *Tetrahedron Lett.* **1997**, *38*, 7295–7298.
9. Bonollo, S.; Lanari, D.; Vaccaro, L. *Eur. J. Org. Chem.* **2011**, *14*, 2587–2598.
10. Smith, J. G. *Synthesis*, **1984**, *8*, 629–656.
11. Cooper, G.; Irwin, W. J. *J. Chem. Soc., Perkin Trans. 1*, **1976**, *5*, 545–549.
12. Kotsuki, H.; Hayashida, K.; Shimanouchi, T.; Nishizawa, H. *J. Org. Chem.* **1996**, *61*, 984–990.
13. Glas, H.; Thiel, W. R. *Tetrahedron Lett.* **1998**, *39*, 5509–5510.
14. Desai, H.; D'Souza, B. R.; Foether, D.; Johnson, B. F.; Lindsay, H. A. *Synthesis*, **2007**, *6*, 902–910.
15. Porcar, R.; Sans, V.; Ríos-Lombardía, N.; Gotor-Fernández, V.; Gotor, V.; Burguete, M. I.; García-Verdugo, E.; Luis, S. V. *ACS Catal.* **2012**, *2*, 1976–1983.
16. Poppe, L.; Novák, L. *Selective Biocatalysis: A Synthetic Approach*, Wiley-VCH, Weinheim, **1992**.
17. Liese, A.; Seelbach, K.; Wandrey, C. (Eds.), *Industrial Biotransformations, 2nd ed.* Wiley-VCH, Weinheim, **2006**.
18. Faber, K. *Biotransformations in Organic Chemistry, 6th ed.* Springer, Berlin-Heilderberg, **2011**.
19. Boros, Z.; Hornyánszky, G.; Nagy, J.; Poppe, L.: Stereoselective hydrolase-catalyzed processes in continuous-flow mode. In *Cascade Biocatalysis: Stereoselective and Environmentally Friendly Reactions*; Riva, S.; Fessner, W. Eds.; Wiley-VCH, Weinheim, **2014** (in press).
20. Bornscheuer, U. T.; Kazlauskas, R. J. *Hydrolases in Organic Synthesis: Regio- and Stereoselective Biotransformations*, Wiley-VCH: Weinheim-New York, **2006**.
21. Schmid, A.; Dordick, J. S.; Hauer, B.; Kiener, A.; Wubbolts, M.; Witholt, B. *Nature*, **2001**, *409*, 258–268.
22. Whittall, J.; Sutton, P. (Eds.), *Practical Methods for Biocatalysis and Biotransformations*, John Wiley & Sons, Ltd., Chichester, **2010**.
23. Dunn, P. J.; Wells, A. S.; Williams M. T. (Eds.), *Green Chemistry in the Pharmaceutical Industry*, Wiley-VCH, Weinheim, **2010**.
24. Busto, E.; Gotor-Fernández, V.; Gotor, V. *Chem. Soc. Rev.* **2010**, *39*, 4504–4523.
25. Humble, M. S.; Berglund, P. *Eur. J. Org. Chem.* **2011**, 3391–3401.
26. Zhou, Z.; Hartmann, M. *Top. Catal.* **2012**, *55*, 1081–1100.
27. Ghanem, A.; Aboul-Enein, H. Y. *Chirality*, **2005**, *17*, 1–15.
28. Ghisalba, O.; Meyer, H. P.; Wohlgemuth, R. "Industrial biotransformations" in *Encyclopedia of Industrial Biotechnology: Bioprocess, Bioseparation, and Cell Technology*, Flickinger, M. C., (Ed.), John Wiley & Sons, Hoboken, **2010**.

29. Hoyos, P.; Pace, V.; Alcántara, A. R. *Adv. Synth. Catal.* **2012**, *354*, 2585–2611.
30. Turner, N. J.; *Curr. Opin. Chem. Biol.* **2004**, *8*, 114–119.
31. Clouthier, M.; Pelletier, J. N. *Chem. Soc. Rev.* **2012**, *41*, 1585–1605.
32. van Rantwijk, F.; Sheldon, R. A.; *Tetrahedron*, **2004**, *60*, 501–519.
33. Garcia-Urdiales, E.; Alfonso, I.; Gotor, V. *Chem. Rev.* **2005**, *105*, 313–354.
34. Sun, J. H.; Dai, R. J.; Meng, W. W.; Deng, Y. L. *Catal. Commun.* **2010**, *11*, 987–991.
35. Poulhès, F.; Vanthuyne, N.; Bertrand, M. P.; Gastaldi, S.; Gil, G. *J. Org. Chem.* **2011**, *76*, 7281–7286.
36. Brem, J.; Bencze, L. C.; Liljeblad, A.; Turcu, M. C.; Paizs, C.; Irimie, F. D.; Kanerva, L. T. *Eur. J. Org. Chem.* **2012**, *17*, 3288–3294.
37. De Miranda, A. S.; Gomes, J. C.; Rodrigues Jr, M. T.; Costa, I. C. R.; Almeida, W. P.; de O. Lopes, R.; Miranda, L. S. M.; Coelho, F.; de Souza, R. O. M. A. *J. Mol. Catal. B: Enzym.* **2013**, *91*, 77–80.
38. Boros, Z.; Falus, P.; Márkus, M.; Weiser, D.; Oláh, M.; Hornyánszky, G.; Nagy, J.; Poppe, L. *J. Mol. Catal. B: Enzym.* **2013**, *85–86*, 119–125.
39. Rouhi A. M. *Chem. Eng. News.* **2004**, *82*, 49–58.
40. Jas, G.; Kirschning, A. *Chem. Eur. J.* **2003**, *9*, 5708–5723.
41. Ceylan, S.; Kirschning, A. In: *Recoverable and Recyclable Catalysts*, Benaglia, M. (Ed.), pp. 379–410. John Wiley & Sons, Ltd., New York, **2009**.
42. Mak, X. Y.; Laurino, P.; Seeberger, P. H. *Beilstein J. Org. Chem.* **2009**, *5*, No. 19.
43. Rasheed, M.; Elmore, S. C.; Wirth, T. In: *Catalytic methods in asymmetric synthesis – Advanced materials, techniques, and applications*, Gruttadauria, M.; Giacalone, F. (Eds.), pp. 345–372. John Wiley & Sons, Inc., Hoboken, **2011**.
44. Yuryev, R.; Strompen, S.; Liese, A. *Beilstein J. Org. Chem.* **2011**, *7*, 1449–1467.
45. *Microreactors in Organic Synthesis, 2nd Ed*, Wirth, T. (Ed.), Wiley-VCH, Weinheim, **2013**.
46. Sheldon, R. A. *Adv. Synth. Catal.* **2007**, *349*, 1289–1307.
47. Mateo, C.; Palomo, J. M.; Fernandez-Lorente, G.; Guisan, J. M.; Fernandez-Lafuente, R. *Enzyme Microb. Technol.* **2007**, *40*, 1451–1463.
48. Hanefeld, U.; Gardossi, L.; Magner, E., *Chem. Soc. Rev.* **2009**, *38*, 453–468.
49. Garcia-Galan, C.; Berenguer-Murcia, A.; Fernandez-Lafuente, R.; Rodrigues, R. C. *Adv. Synth. Catal.* **2011**, *353*, 2885–2904.
50. Sheldon, R. A.; van Pelt, S. *Chem. Soc. Rev.* **2013**, *42*, 6223–6235.
51. Rodrigues, R. C.; Ortiz, C.; Berenguer-Murcia, A.; Torres, R.; Fernández-Lafuente, R. *Chem. Soc. Rev.* **2013**, *42*, 6290–6307.
52. Lam, L. K. P.; Hui, R. A.; Jones, J. B. *J. Org. Chem.* **1986**, *51*, 2047–2050.
53. Rantakylä, M.; Aaltonen, O. *Biotechnol. Lett.* **1994**, *16*, 825–830.
54. Molinari, F.; Mantegazza, L.; Villa, R.; Aragozzini, F. *J. Ferment. Bioeng.* **1998**, *86*, 62–64.
55. Ljubović, E.; Majerić-Elenkov, M.; Avgadić, A.; Šunjić, V. *Food Technol. Biotechnol.* **1999**, *37*, 215–224.
56. López-Serrano, P.; Wegman, M. A.; van Rantwijk, F.; Sheldon, R. A. *Tetrahedron Asymmetry*, **2001**, *12*, 235–240.
57. Cainelli, G.; Galletti, P.; Giacomini, D.; Gualandi, A.; Quintavalla, A. *Helv. Chim. Acta*, **2003**, *86*, 3548–3559.
58. Sakai, T. *Tetrahedron: Asymmetry*, **2004**, *15*, 2749–2756.
59. Moon-Young, Y.; Lee, S. H.; Cheong, C. S.; Park, J. K. *Enzyme Microb. Technol.* **2004**, *35*, 574–580.
60. Chen, C. C.; Tsai, S. W.; *Enzyme Microb. Technol.* **2005**, *36*, 127–132.
61. Lin, C.; Hiraga, Y.; Masaki, K.; Iefuji, H.; Ohkata, K. *Biocatal. Biotransform.* **2006**, *24*, 390–395.
62. Yang, G.; Wu, J.; Xu, G.; Yang, L. *Appl. Microbiol. Biotechnol.* **2009**, *81*, 847–853.
63. Cipiciani, A.; Bellezza, F.; Fringuelli, F.; Silvestrini, M. G. *Tetrahedron: Asymmetry*, **2001**, *12*, 2277–2281.
64. Magnusson, A. O.; Takwa, M.; Hamberg, A.; Hult, K. *Angew. Chem. Int. Ed.* **2005**, *44*, 4582–4585.
65. Csajági, C.; Szatzker, G.; Töke, E. R.; Úrge, L.; Darvas, F.; Poppe, L. *Tetrahedron: Asymmetry*, **2008**, *19*, 237–246.
66. Barton, M. J.; Hamman, J. P.; Fichter, K. C.; Calton, G. J. *Enzyme Microb. Technol.* **1990**, *12*, 577–583.
67. Gharpure, S. J.; Sathiyarayanan, A. M. *Chem. Commun.* **2011**, *47*, 3625–3627.
68. Chen, C. S.; Fujimoto, Y.; Girdaukas, G.; Sih, C. J. *J. Am. Chem. Soc.* **1982**, *104*, 7294–7299.
69. Boros, Z.; Abaháziová, E.; Oláh, M.; Sátorhelyi, P.; Erdélyi, B.; Poppe, L. *Chim. Oggi*, **2012**, *30*, 26–29.
70. Choi, E.; Kim, Y.; Ahn, Y.; Park, J.; Kim, M. *Tetrahedron: Asymmetry*, **2013**, *24*, 1449–1452.

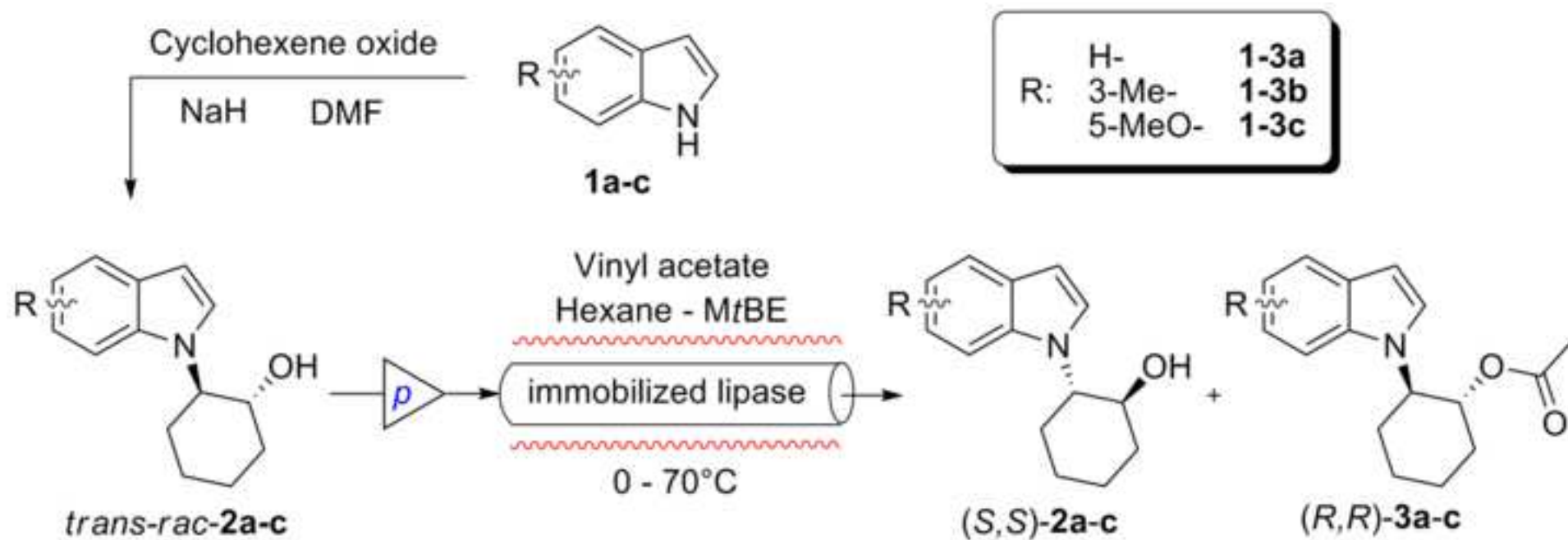


Figure 1  
[Click here to download high resolution image](#)

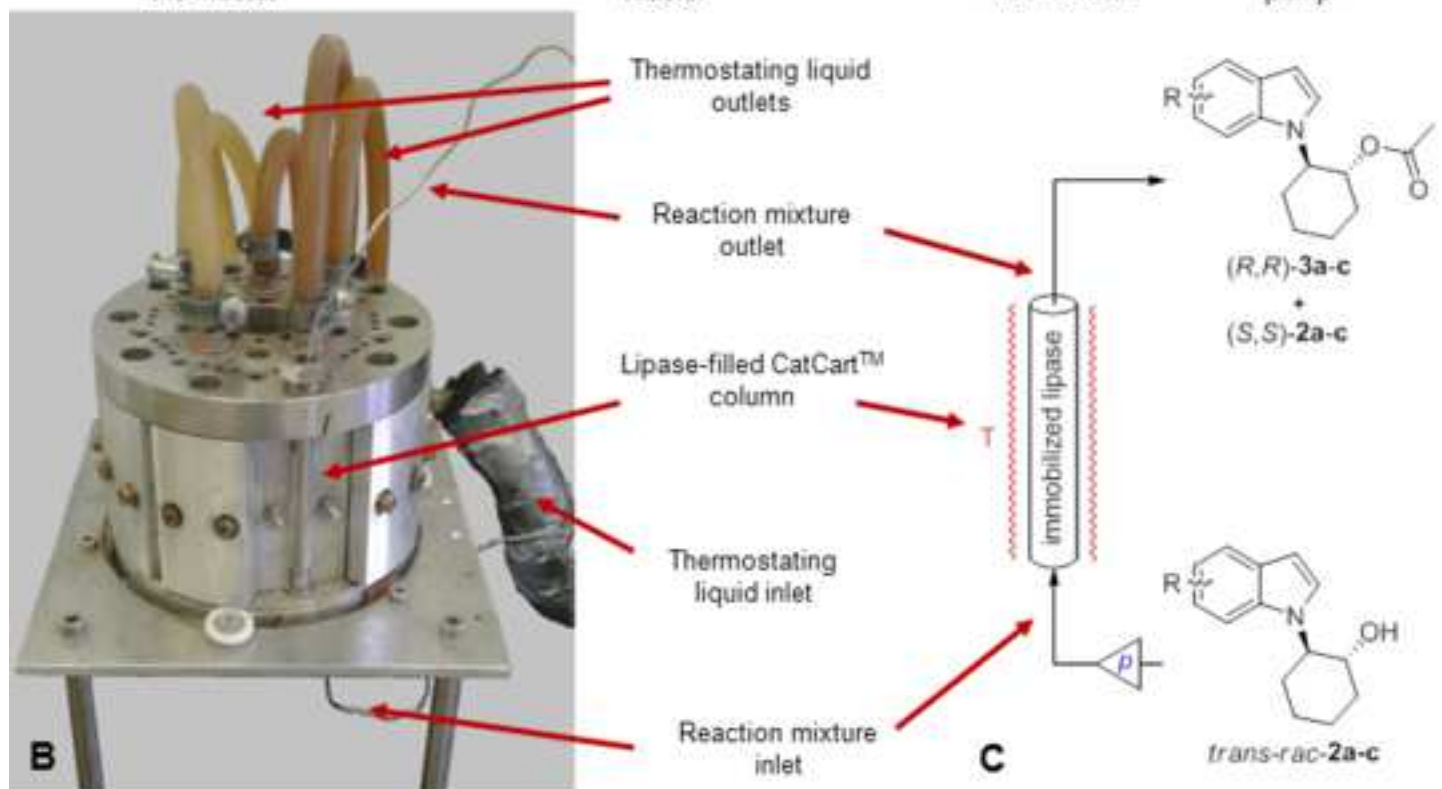
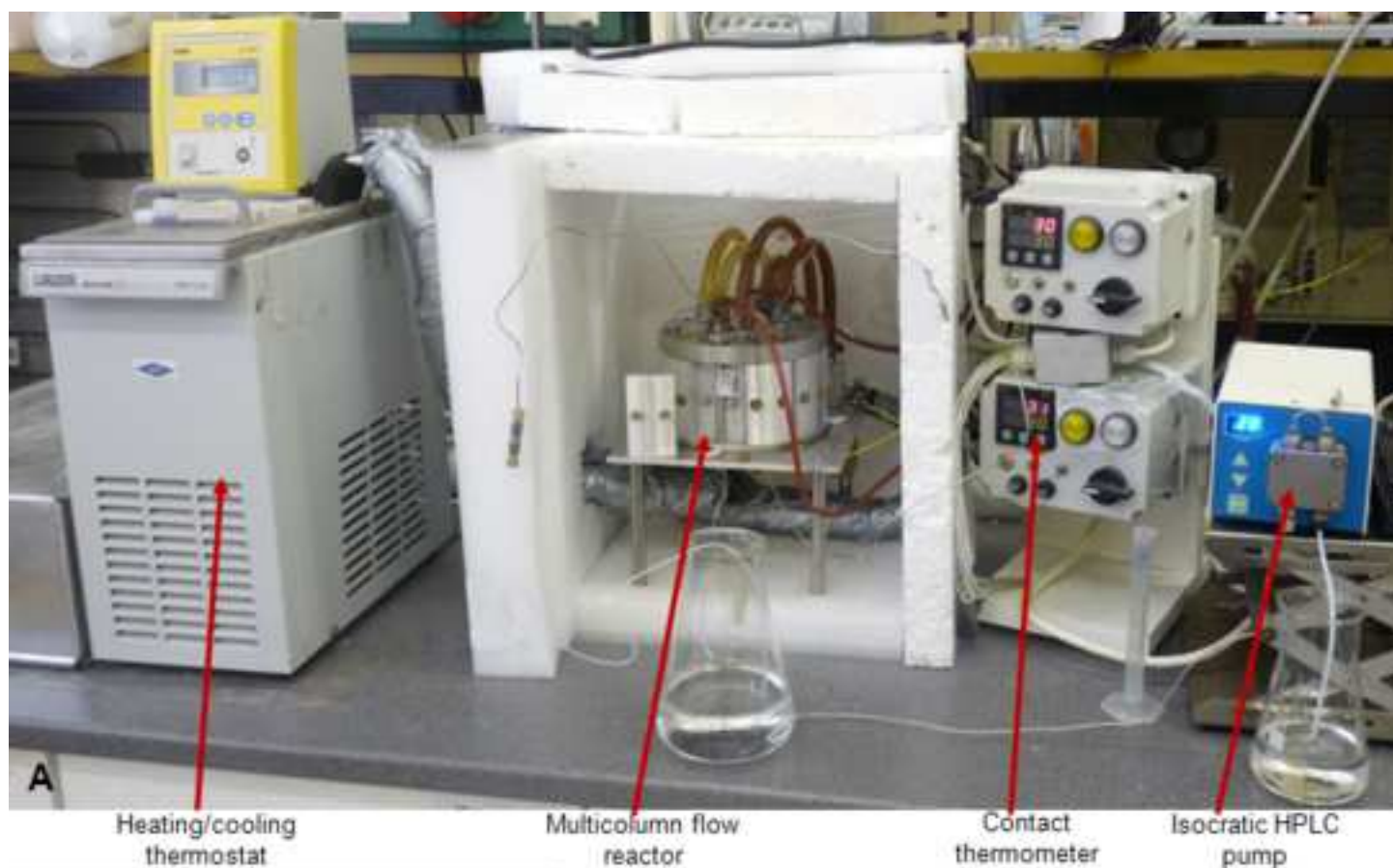


Figure 2  
[Click here to download high resolution image](#)

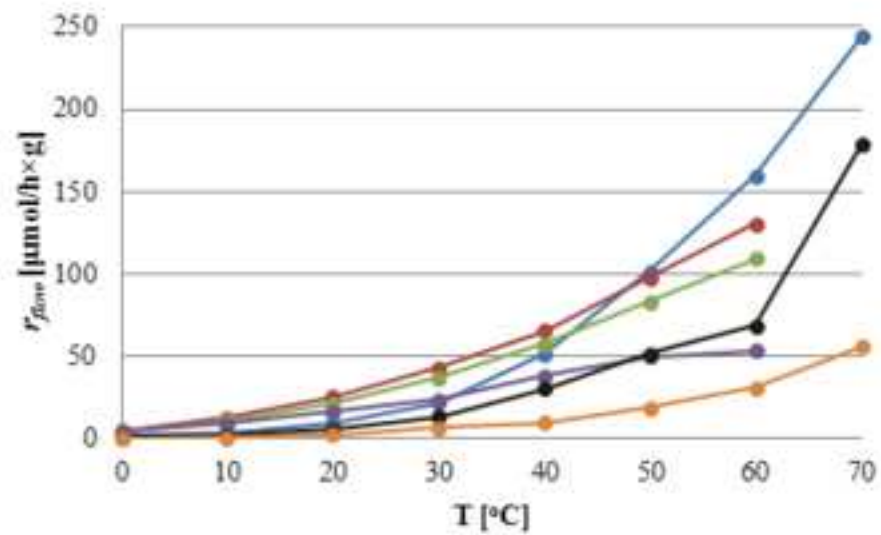
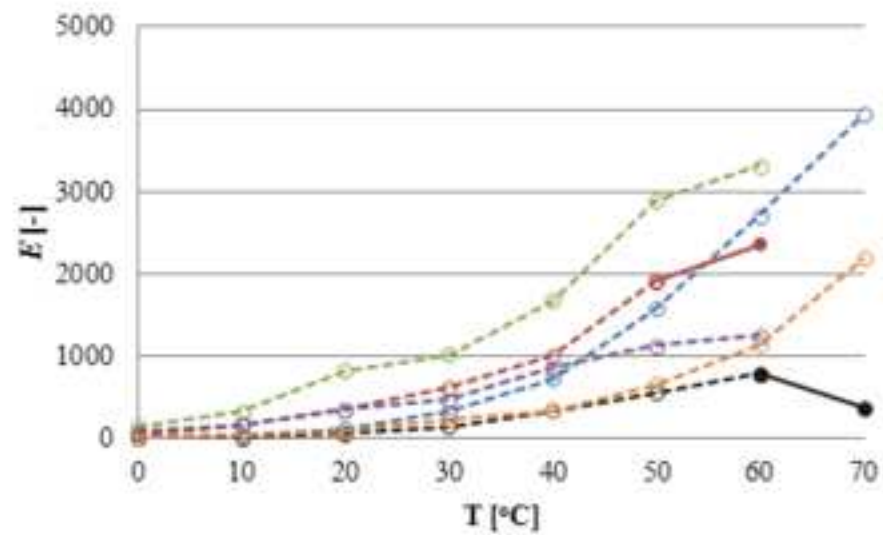
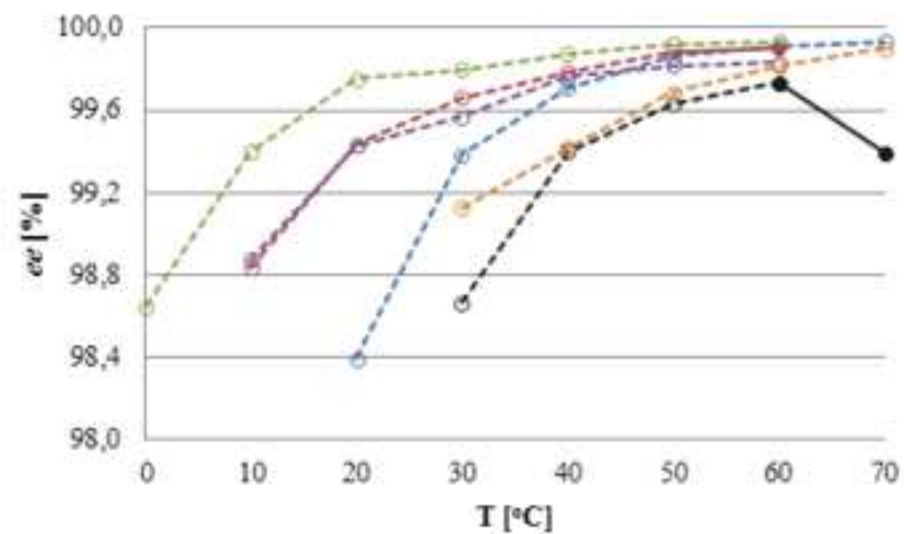
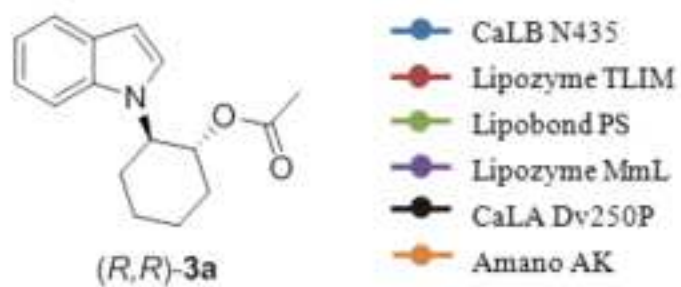




Figure 3  
[Click here to download high resolution image](#)

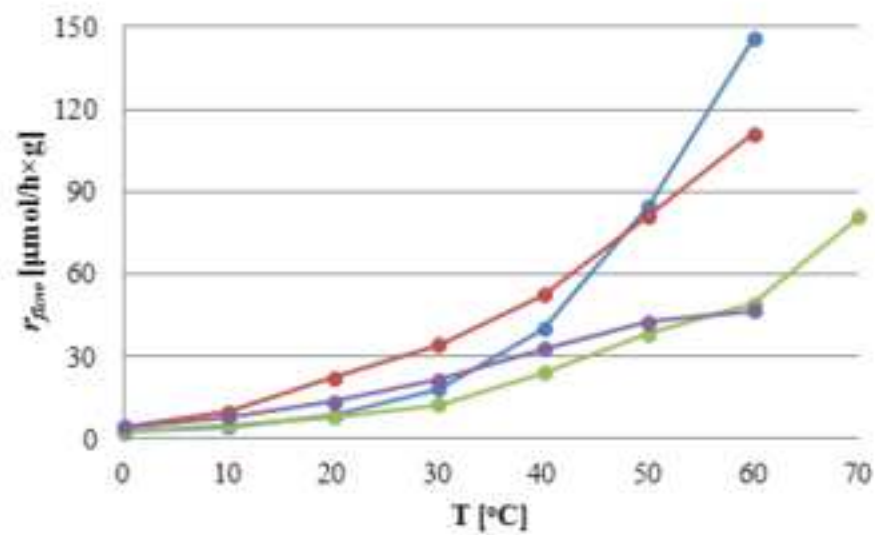
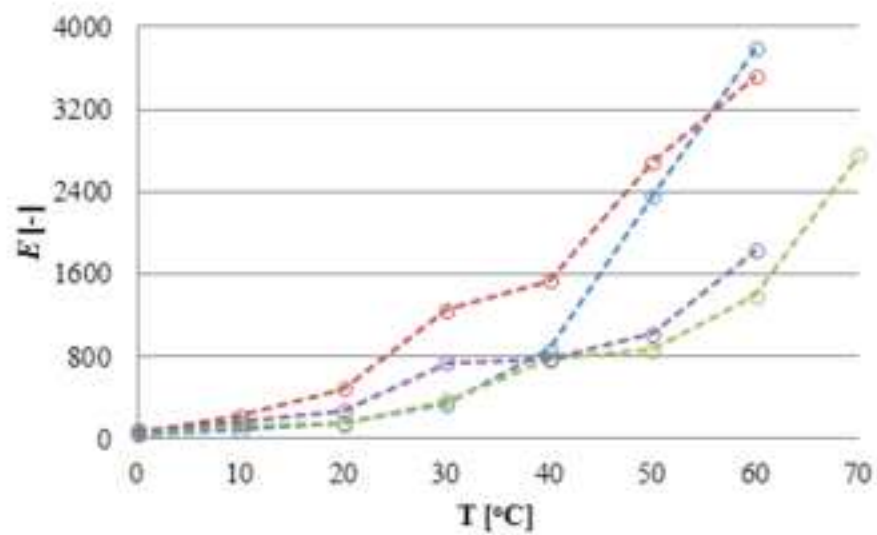
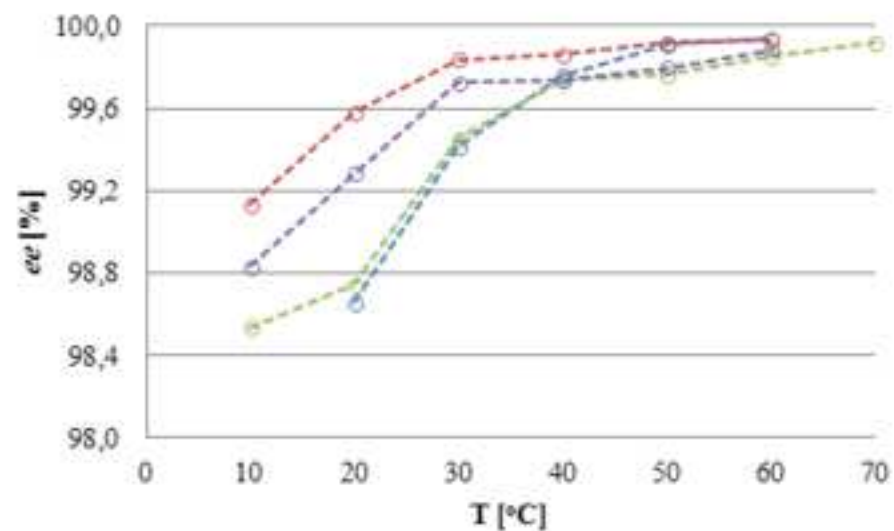
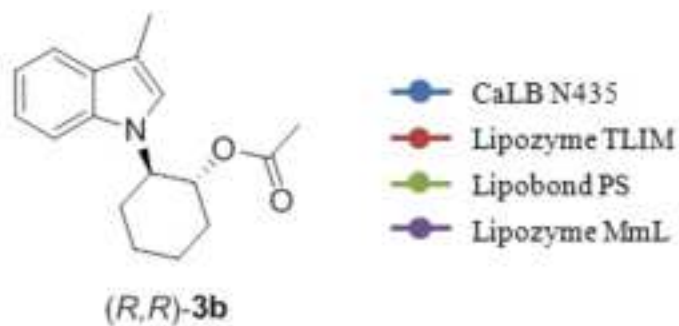
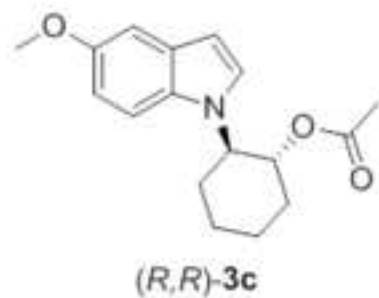
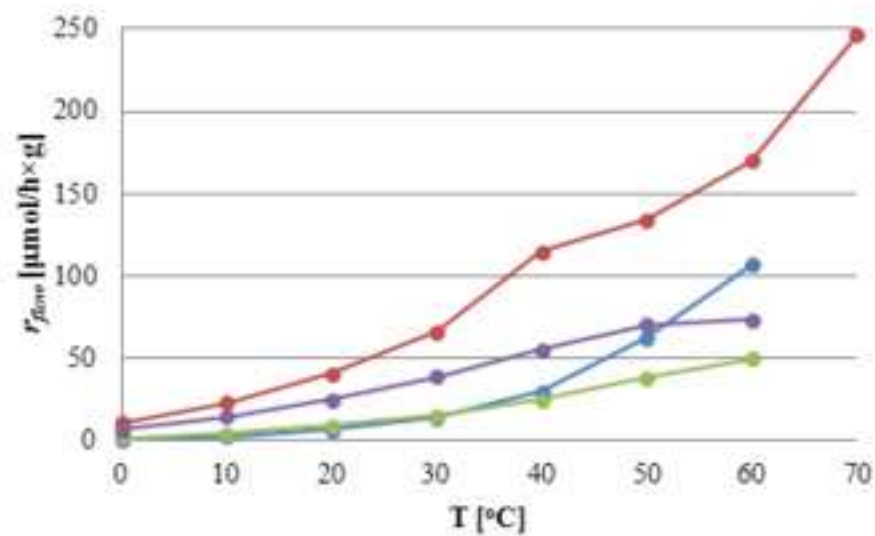
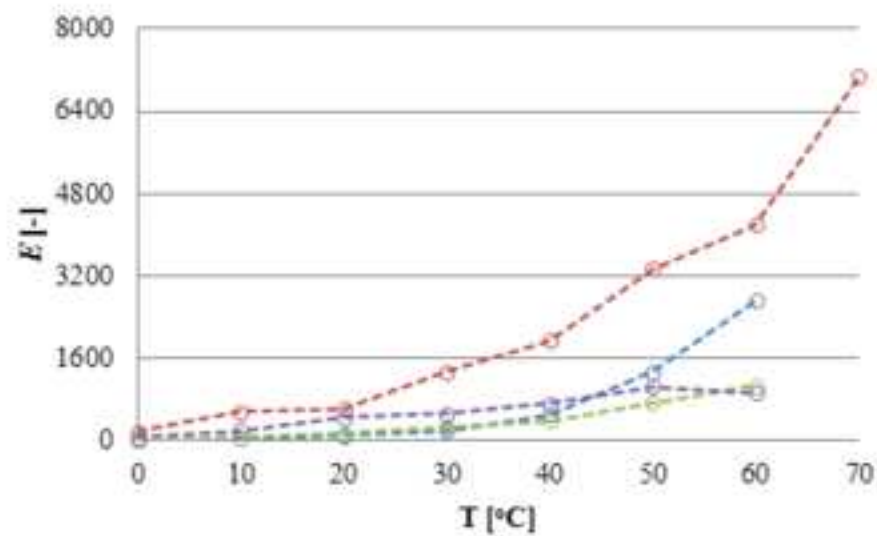
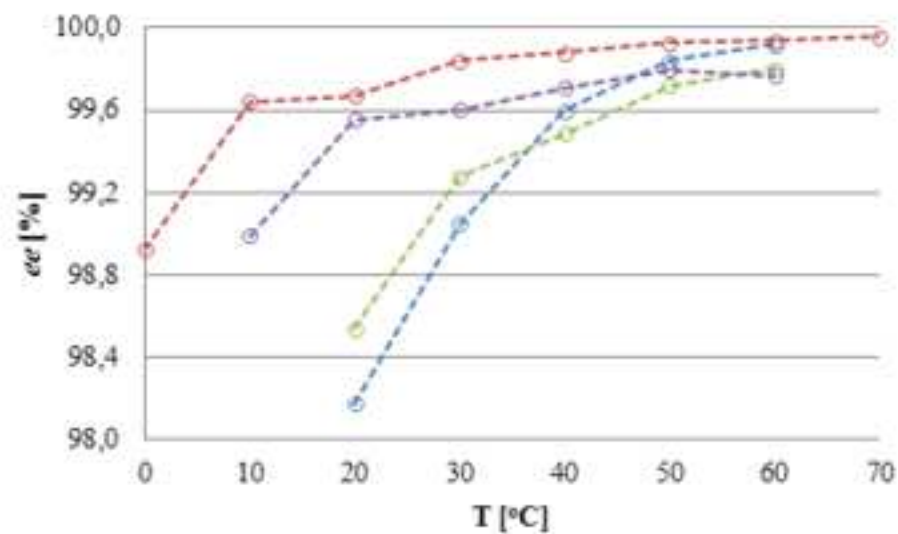
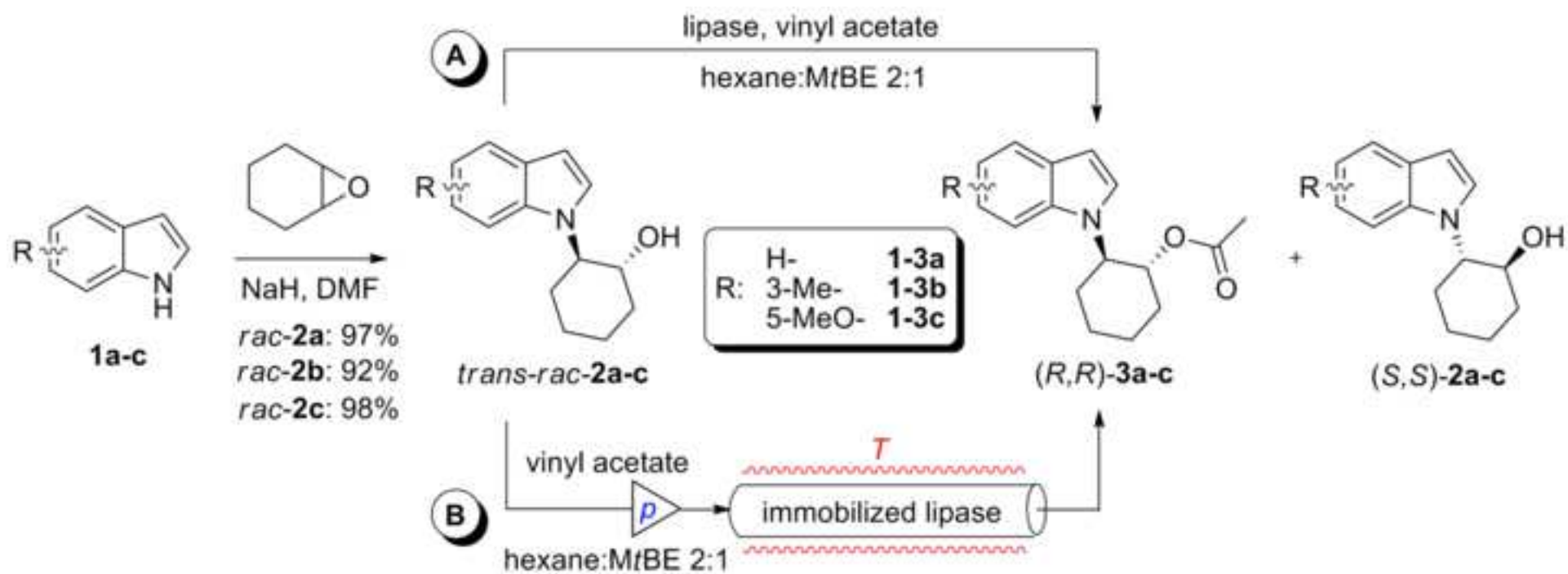


Figure 4  
[Click here to download high resolution image](#)



- CaLB N435
- Lipozyme TLIM
- Lipobond PS
- Lipozyme MmL





**Table 1.** Lipase-catalysed kinetic resolution of secondary alcohols (*rac*-**2a–c**) by acylation with vinyl acetate in batch mode (30°C, shake flask).

Entry	Substrate	Enzyme	<i>c</i> (%) <sup>a</sup>	<i>ee</i> <sub>(<i>R,R</i>)-<b>3a–c</b></sub> (%) <sup>b</sup>	<i>E</i> <sup>c</sup>	<i>r</i> <sub>batch</sub> (μmol g <sup>-1</sup> h <sup>-1</sup> )
Panel A <sup>d</sup>						
1	<i>rac</i> - <b>2a</b>	CaLB N435	49.9	>99.9	»200	32.6
2	<i>rac</i> - <b>2a</b>	Lipobond PS	47.2	>99.9	»200	30.8
3	<i>rac</i> - <b>2a</b>	Lipozyme TLIM	40.2	>99.9	»200	26.2
4	<i>rac</i> - <b>2a</b>	Lipozyme MmL	38.7	>99.9	»200	25.3
5	<i>rac</i> - <b>2a</b>	Amano AK	37.0	>99.9	»200	24.1
6	<i>rac</i> - <b>2a</b>	CaLA G250P	25.1	99.8	»200	16.4
7	<i>rac</i> - <b>2a</b>	CaLA T2-150	14.7	99.6	»200	9.6
8	<i>rac</i> - <b>2a</b>	MpL G250P	13.9	99.9	»200	9.0
9	<i>rac</i> - <b>2a</b>	MpL G250O	11.1	99.9	»200	7.2
10	<i>rac</i> - <b>2a</b>	CaLB G250P	9.4	99.9	»200	6.2
11	<i>rac</i> - <b>2a</b>	PaL G250P	8.6	99.8	»200	5.6
Panel B <sup>e</sup>						
12	<i>rac</i> - <b>2b</b>	CaLB N435	41.2	>99.9	»200	37.6
13	<i>rac</i> - <b>2b</b>	Lipobond PS	27.7	>99.9	»200	25.0
14	<i>rac</i> - <b>2b</b>	Lipozyme TLIM	27.4	>99.9	»200	25.0
15	<i>rac</i> - <b>2b</b>	Lipozyme MmL	24.1	>99.9	»200	21.7
16	<i>rac</i> - <b>2b</b>	CaLB G250P	12.9	99.9	»200	11.9
17	<i>rac</i> - <b>2b</b>	Amano AK	9.0	99.9	»200	8.1
18	<i>rac</i> - <b>2b</b>	Amano M	6.5	99.9	»200	5.9
19	<i>rac</i> - <b>2b</b>	Amano PS	5.5	99.8	»200	5.0
Panel C <sup>e</sup>						
20	<i>rac</i> - <b>2c</b>	Lipozyme TLIM	44.9	>99.9	»200	38.6
21	<i>rac</i> - <b>2c</b>	CaLB N435	38.7	>99.9	»200	33.0
22	<i>rac</i> - <b>2c</b>	Lipozyme MmL	34.4	>99.9	»200	29.1
23	<i>rac</i> - <b>2c</b>	Lipobond PS	33.5	>99.9	»200	28.5
24	<i>rac</i> - <b>2c</b>	Amano AK	27.0	99.9	»200	22.8
25	<i>rac</i> - <b>2c</b>	CaLB G250P	13.7	99.9	»200	11.7
26	<i>rac</i> - <b>2c</b>	CaLA G250P	10.6	99.9	»200	9.0
27	<i>rac</i> - <b>2c</b>	CrL	7.3	99.9	»200	6.2
28	<i>rac</i> - <b>2c</b>	Amano PS	7.2	99.8	»200	6.1
29	<i>rac</i> - <b>2c</b>	CaLA T2-150	6.9	99.8	»200	5.9

<sup>a</sup> Results are shown only for reactions with *c* >5%.<sup>b</sup> Enantiomeric excess of ester (*ee*<sub>(*R,R*)-**3a–c**</sub>) was determined by chiral GC.<sup>c</sup> Enantiomeric ratio (*E*) was calculated from *c* and *ee*<sub>(*R,R*)-**3a–c**</sub>.<sup>68</sup> For simplicity, *E* values calculated above 500 were given as »200.<sup>d</sup> Reaction time 72 h.<sup>e</sup> Reaction time 48 h.<sup>68</sup> Chen, C. S.; Fujimoto, Y.; Girdaukas, G.; Sih, C. J. *J. Am. Chem. Soc.* **1982**, *104*, 7294–7299.

**Table 2.** Alcohols prepared by kinetic resolution of *rac*-**2a–c** with vinyl acetate in a CaLB N435-filled continuous-flow reactor at preparative scale followed by Zemplén deacylation of the formed (*R,R*)-**3a–c**.

Compound	Yield (%)	<i>ee</i> (%) <sup>a</sup>	$[\alpha]_D^{26}$ <sup>c,b</sup>
( <i>R,R</i> )- <b>2a</b>	36 <sup>c</sup>	97.8	+0.86
( <i>S,S</i> )- <b>2a</b>	39	87.9	−0.75
( <i>R,R</i> )- <b>2b</b>	33 <sup>c</sup>	98.1	+0.17
( <i>S,S</i> )- <b>2b</b>	34	94.8	−0.07
( <i>R,R</i> )- <b>2c</b>	35 <sup>c</sup>	98.7	+0.47
( <i>S,S</i> )- <b>2c</b>	33	93.1	−0.19
( <i>R,R</i> )- <b>3a</b>	45	99.1	+12.7
( <i>R,R</i> )- <b>3b</b>	43	99.5	+10.7
( <i>R,R</i> )- <b>3c</b>	42	99.2	+11.8

<sup>a</sup> Enantiomeric excess was determined by chiral GC (see Section 4.2).<sup>b</sup> Specific rotations, (*c* 1.0, CH<sub>2</sub>Cl<sub>2</sub>).<sup>c</sup> Combined yield of kinetic resolution and Zemplén deacylation.